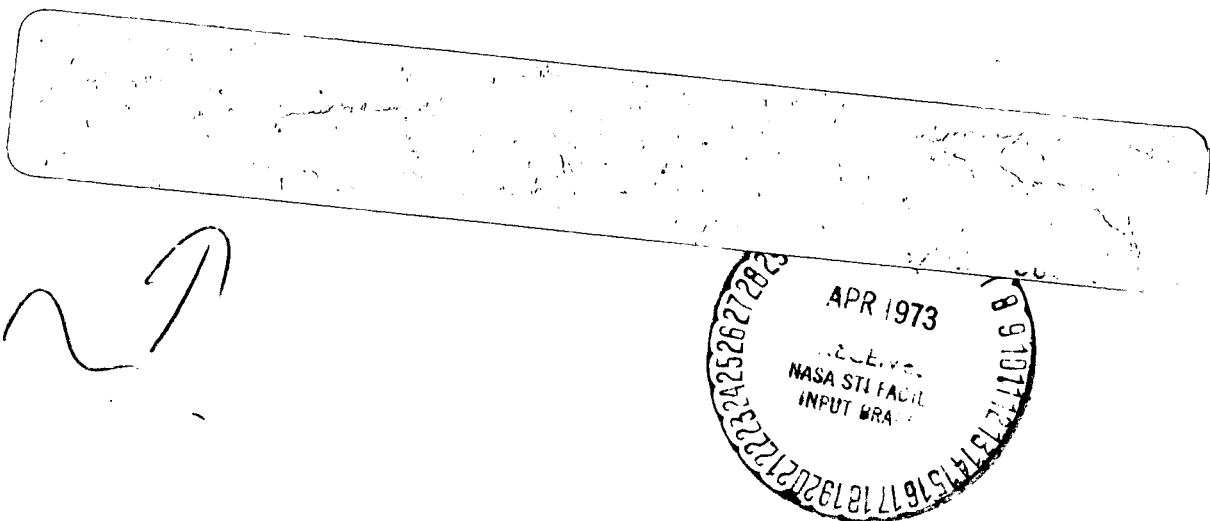


2
~~114576~~
AVAILABLE TO U.S. GOVT.
~~AMERICAS ONLY~~
(NASA-CR-114576) ANALYTICAL LIFT FAN
NOISE STUDY Interim Report, 13 Apr.
1971 - 13 June 1972 (Rao (G. V. R.) and
Associates) 78 p HC \$6.00 CSCL 01C

N73-30952

Unclassified
G3/02 14743



G.V.R. RAO AND ASSOCIATES

14827 VENTURA BOULEVARD, SHERMAN OAKS, CALIF. 91403

G. V. R. RAO AND ASSOCIATES
AERODYNAMICS AND PROPULSION
TECHNOLOGY
14827 VENTURA BOULEVARD
SHERMAN OAKS, CALIFORNIA 91403
TELEPHONE (213) 981-5644

Interim Report

Analytical Lift Fan Noise Study

Contract No. NAS2-6401

Prepared by:

Dr. G. V. R. Rao
Dr. Wing T. Chu
R. V. Digumarthi

July 13, 1972

Z

SUMMARY

This interim report presents the investigations carried out by G. V. R. Rao and Associates during the period April 13, 1971, to June 13, 1972, under Contract No. NAS2-6401 with National Aeronautics and Space Administration, Ames Research Center, Moffet Field, California. Based on reasonable estimates of flow conditions occurring in an axial fan, acoustic radiation from various noise sources is evaluated. Results of computations on two specific fans are presented, and relative significance of the various sources is examined. The information presented here constitutes a step in our continuing effort on understanding fan noise. Helpful suggestions from Mr. David Hickey and Mr. Brent Hodder of Large Scale Aerodynamics Branch are greatly appreciated.

TABLE OF CONTENTS

	<i>page</i>
SUMMARY	i
NOMENCLATURE	iii
I INTRODUCTION	1
II DIPOLE SOURCES IN AN AXIAL FAN	5
A. Steady State Loading on Rotor Blades	5
B. Unsteady Loading on Rotor Blades	8
1. Periodic Fluctuations in Rotor Blade Load	8
2. Random Fluctuation in Rotor Blade Load	14
C. Unsteady Loading on Stator Vanes	17
1. Periodic Fluctuation in Stator Vane Load	17
2. Random Fluctuation in Stator Vane Load	23
III QUADRUPOLE SOURCES IN AN AXIAL FAN	24
A. Description of Flow Field	24
1. Steady State Mean Flow	25
2. Perturbations from Potential Flow	26
3. Perturbations Due to Velocity Deficit in the Wakes	28
4. Random Velocity Fluctuation in Turbulent Regions	31
B. Ordered Quadrupoles Due to Periodic Velocity Fluctuations	34
1. Effect of Rotor Related Flow Field	34
2. Effect of Stator Related Flow Field	38
C. Random Quadrupoles Due to Inflow Turbulence	42
1. Effect of Rotor Potential Flow Field	42
2. Effect of Rotor Wakes	45
3. Effect of Stator Flow Field	46
D. Random Quadrupoles Due to Turbulence in the Wake Regions	46
IV CONCLUDING REMARKS AND RECOMMENDATIONS	47
REFERENCES	50
FIGURES	53

NOMENCLATURE

B	number of blade elements
C_L	section lift coefficient
F_i	components of the externally applied forces on the fluid boundary ($i = 1, 2, 3$)
J	Bessel function of the first kind
M	Mach number
M_a	Mach number of the axial component of the steady state mean flow
M_t	rotor tangential velocity divided by the ambient speed of sound
N	revolutions per second (speed of the rotor)
R	distance of the field point from the fan center
T_{ij}	components of the externally applied stress distributed within the fluid volume ($i, j = 1, 2, 3$)
U	velocity
U_a	axial flow velocity through the fan
U_c	convective velocity of the "frozen convective pattern" model of turbulence
U_i	velocity component ($i = 1, 2, 3$)
U_n	velocity component normal to the fluid boundary
U_o	mean flow velocity
U_t	rotor tangential velocity
V	number of vanes in stator
V_o	mean flow velocity relative to rotor or stator
X_i	fixed cartesian coordinate system with its origin at the fan center ($i = 1, 2, 3$)

a	an index
a_o	ambient speed of sound
c	chord length
d	circumferential spacing of blades or vanes
d_p	circumferential spacing of rotor blade at pitch radius
h	distance from the source
k	vane number
ℓ	length scale of turbulence
m	an index
n	harmonic index (=1 for blade passing frequency)
r	radial distance from the fan center
v	random fluctuations in velocity
x_i	cartesian coordinate ($i = 1,2,3$) with origin at the source
x'	axial distance upstream of leading edge
x''	axial distance downstream of trailing edge
ΔL	lift per unit span on rotor blade or stator vane
Δp	contribution from elemental annulus to radiated acoustic field
(δv)	velocity deficit in the wake
$(\delta v)^0$	velocity deficit at the wake center line
Φ_L	power spectrum of random fluctuating lift per unit span of blade
Φ_p	power spectrum of radiated acoustic field
Φ_Q	power spectrum of elemental quadrupole source
Φ_{v_0}	power spectrum of the axial component of turbulent fluctuations in the inflow

$\Phi_{v_{0n}}$	power spectrum of the component normal to blade chord of turbulent fluctuations in the inflow
ψ	aspect angle of the field point measured from the fan axis
Ω	circular frequency of rotor rotation
β_1	number of blade crossings during eddy lifetime
β_3	number of blades experiencing simultaneous velocity fluctuations
θ	polar angle measured from the reference meridional plane
λ	stagger angle
ν	angle between wake center line and normal to the elemental annulus
ξ	axial distance of the source from the fan center
ρ	density
ρ_0	ambient density
ϕ	phase angle
ψ_w^r	circumferential location of the OGV wake at the annulus under consideration from reference meridional plane
ψ_w^s	circumferential location of the IGV wake at the annulus under consideration from reference meridional plane
ω	circular frequency
subscripts	
a	ath component
h	at hub location of the fan
i,j	components in the three dimensional cartesian coordinate directions (i,j = 1,2,3)

m mth component
n nth harmonic component
p due to potential flow
r rotor related quantity
s stator related quantity
t at the tip location of the fan
w due to viscous wakes
1,2,3 components in axial, radial and tangential directions
(1) fundamental component

superscripts

— temporal mean
— root mean square value
.. $\partial^2 / \partial t^2$
^ amplitude (absolute value)

special symbols

^
() amplitude
[] function evaluated at retarded time

I. INTRODUCTION

The radiated noise from an axial fan is a by-product of airflow past the moving and stationary elements in the fan. If the velocity field is known, or can be appropriately estimated, one can evaluate the pressure fluctuations in the far field. Based on the work of Lighthill (1) and Curle (2) the pressure fluctuations caused by propagation of aerodynamically generated sound can be written in the form

$$p - p_0 = \frac{1}{4\pi} \frac{\partial^2}{\partial x_i \partial x_j} \int_V \left[\frac{T_{ij}}{h} \right] dv - \frac{1}{4\pi} \frac{\partial}{\partial x_i} \int_S \left[\frac{F_i - \rho U_i U_n}{h} \right] ds - \frac{1}{4\pi} \int_S \frac{\partial}{\partial t} \left[\frac{\rho U_n}{h} \right] ds \quad (1)$$

where p = acoustic pressure in the far field

ρ = density

p_0 = ambient pressure

x_i = cartesian coordinates ($i=1,2,3$) with origin at the source

F_i = components of the externally applied forces on the fluid boundary

T_{ij} = components of the externally applied stresses distributed within the fluid volume

U_i = velocity components

and h = distance from the source.

The subscripts i and j in the above equation indicate components in the three dimensional cartesian coordinate directions and repeated index denotes Einstein summation

convention. The subscript n denotes the component normal to the fluid boundary. The square brackets indicate that the quantities are evaluated at retarded times.

The significance and interpretation of the various terms of Eq. (1) are discussed in ref. (3). The first term on the right hand side of Eq. (1) is from quadrupole sources within the fluid volume. Ffowcs Williams, in ref. (4), indicated that the quadrupole stress density T_{ij} can be approximated by $\rho U_i U_j$. The second term in Eq. (1) represents the dipole sources located on the fluid boundary. These dipole sources consist of exerted forces F_i and the momentum $\rho U_i U_n$ transferred to the fluid when the boundary moves with a velocity U_n normal to itself. The last term is from monopole sources resulting from displacement of the fluid by the motion of the boundary.

The coordinates x_i ($i=1,2,3$) and distance h appearing in Eq. (1) can be related to R , the distance of the field point from fan center and ψ , the aspect angle measured from fan axis. It is convenient to choose the center of the rotor plane as fan center. As shown in enclosed Fig. (1), let us choose a fixed cartesian coordinate system X_1, X_2, X_3 with its origin at the fan center, and $X_2 X_3$ plane containing the field point (R, ψ) . Let r, θ, ξ denote the cylindrical coordinates of the source, which may be any one of the types described above. The radial distance from fan center is denoted r , whereas θ denotes the angle between the $X_2 X_3$ plane and the meridional plane

containing the source point. The axial distance of the source point from fan center is denoted ξ . In the discussions presented in later sections θ is considered positive when measured in the direction of rotor rotation. The cartesian coordinate system 1,2,3 with its center at the source point, are conveniently taken in the axial, radial and tangential directions as shown in the figure. By appropriate translation and rotation of the coordinate system we can derive the following relations.

$$\begin{aligned}
 x_1 &= R\cos\psi - \xi \\
 x_2 &= R\sin\psi\cos\theta - r \\
 x_3 &= -R\sin\psi\sin\theta \\
 \text{and } h &\approx R \left\{ 1 - \frac{2r}{R} \sin\psi\cos\theta + \frac{r^2}{R^2} \right\}^{\frac{1}{2}}
 \end{aligned} \tag{2}$$

In far field computations of fan noise the second order term in (r/R) can be ignored.

In applying Eq. (1) to evaluate the effect the various acoustic sources present in an axial fan we shall adopt the following approach. The various elements in the fan, such as rotor blades, stator vanes and support struts form the fluid boundaries. Also these elements set up a velocity field extending into the fluid volume. Each row of blades, or vanes, or struts can be replaced by a fictitious actuator disc, with the flow parameters and forces appropriately prescribed on them. The flow field set up by the blades or vanes is considered to influence the quadrupole strength distribution within the fluid on either side of the actuator disc.

In this interim report we have considered only the quadrupole sources within the fluid and the externally applied forces on the boundaries. The influence of the remaining terms of Eq. (1) is presently under consideration and will be treated in a later report. Only such acoustic sources that contribute to the noise at blade passing frequency and its harmonics are examined in this report, since such discrete frequency noise is the prime origin of annoyance. In our preliminary evaluation of fan noise, we have ignored the influence of the duct walls. Consequently, the only boundaries of the fluid considered are actuator discs replacing the rotor and stator. Such omission is a valid approximation, if we restrict our attention only to the propagating modes in the duct as discussed by Tyler and Soffrin (5).

II. DIPOLE SOURCES IN AN AXIAL FAN

From the airfoil section characteristics and mean flow properties, the aerodynamic loads on the various blade or vane elements can be obtained. The forces acting at the discrete locations of these elements can be distributed over appropriate cross sectional planes by employing Fourier representation. Besides the steady state load, the rotor blades will experience periodic fluctuating loads as they cross the wakes from upstream stator vanes and also random forces due to turbulence in the flow. The vanes in a stator located downstream of the rotor also experience similar steady and unsteady loads. In evaluating acoustic radiation from such dipole sources, the influence of the blades and vanes can be replaced by an equivalent distribution of dipole sources in the rotor and stator planes respectively.

II.A. Steady State Loading on Rotor Blades

Let us consider B number of blade elements equally spaced in an annulus $2\pi r dr$ of the fan cross section. Each blade element experiences a force given by

$$\Delta L = \frac{\rho}{2} V_o C_{Lr} c_r dr \quad (3)$$

where V_o = mean flow velocity relative to the rotor blade

C_{Lr} = rotor blade section lift coefficient

and c_r = rotor blade chord.

In the above representation we have ignored the drag compared to the lift on the blade element. Since the force ΔL acts essentially normal to the blade chord, we can write the axial and tangential components as

$$\Delta L_1 = \Delta L \sin \lambda_r$$

$$\text{and } \Delta L_3 = \Delta L \cos \lambda_r$$

where λ_r = the rotor blade stagger angle.

The lift ΔL acting on each blade element can be considered concentrated at the center of pressure of the blade element. An equal and opposite force is exerted on the fluid. As the blades rotate at an angular velocity Ω , we obtain a fluctuating force distribution on the annulus which can be represented by the real part of a complex Fourier series as

$$dF = - \sum_{n=1}^{\infty} \frac{\Delta L}{\pi} B e^{i(nB\theta - ka_0 t)} \quad (4)$$

where n = harmonic index (=1 for blade passing frequency)

$$ka_0 = n \Omega B$$

$$\Omega = 2\pi N$$

and N = rotor revolutions per second.

In the above simple representation we observe that the amplitude and phase angle of each harmonic are the same, as a consequence of assuming ΔL as concentrated at a point. Consideration of chord-wise distribution of ΔL , and its effect on loading harmonics is discussed in ref. (6). Amplitudes in higher harmonics would then fall off rapidly.

The term ΔL in Eq. (4), as described by Eq. (3), is dependent upon the flow conditions and blade section characteristics occurring at the radius r under consideration. For the design conditions on Rao Fan 2, described in ref. (7), the radial variation of ΔL is shown in Fig. (2). The blade loading on LF336 fan, described in ref. (8), operating at design conditions is presented in Fig. (3).

Acoustic radiation field from the forces described by Eq. (4), acting on the elemental annulus $2\pi r dr$, can be obtained by using the second term on the right hand side of Eq. (1). Upon integration over θ , from 0 to 2π , the rms value of the nth harmonic of sound pressure can be written as

$$\tilde{A}p_n = \frac{k_B}{2\sqrt{2\pi}R} \Delta L \left| \sin \lambda_r \cos \psi - \frac{nB}{kr} \cos \lambda_r \right| J_{nB}(krsin\psi) \quad (5)$$

where J_{nB} is the Bessel function of the first kind of order nB and argument $krsin\psi$, and ΔL is given by Eq. (3).

The above equation for acoustic radiation from an elemental annulus $2\pi r dr$ containing B number of rotor blades, is the same as that derived several years ago by Gutin (9). Substituting Eq. (3) for ΔL into the right hand side of above Eq. (5) and integrating from $r = r_h$ to r_t , one obtains the radiated sound pressures from the steady state rotor blade loading. The results of such computations at the blade passing frequency on the two fans referred above are shown in Figs. (4) and (5) respectively. As can be expected from multibladed rotors, the theoretical estimates presented in Figs. (4) and

(5) are far below the measured values given in refs. (7) and (8). Filleul in ref. (10), also indicated the inadequacy of steady state rotor blade loading for predicting noise from rotors with large number of blades.

II.B. Unsteady Loading on Rotor Blades

As the rotor blades travel circumferentially, they encounter non-uniform flow conditions. In the following analysis we shall restrict our attention to the circumferentially non-uniform steady flow caused by upstream vanes and also the random fluctuations in velocity. The former gives rise to periodic fluctuations in blade loading, which can be treated as "ordered" dipoles on rotor blades in the acoustic calculations. On the other hand, the random velocity fluctuations present in the turbulent regions give rise to random dipole sources on the blades. Acoustic radiation from such ordered and random sources are examined in this section.

II.B.1. Periodic Fluctuation in Blade Loading

Circumferential steady non-uniformity in the flow met by a rotor, due to inflow distortion or the presence of upstream stator vanes, causes periodic fluctuations in blade loading. Steady state inflow distortion, met by a blade, is repeated in each revolution of the rotor and hence the fundamental of the resulting periodic blade loading is the rotor frequency. On the other hand, in the case of an upstream stator causing N number of identical wakes, the rotor blade experiences

periodic loading with a fundamental frequency NV . Let us examine the latter case in detail, since similar analysis also applies to the effect of inflow distortion.

A method of estimating the lift fluctuations on the blade elements is discussed in ref. (11), and can be represented by the real part of a complex Fourier series as

$$\Delta L = \sum_{a=-\infty}^{\infty} (\Delta L)_a \hat{e}^{-i\phi_a} e^{-iaV\Omega t} \quad (6)$$

The amplitude $(\Delta L)_a$ and the phase angle ϕ_a of each a th component depend upon frequency, wake-velocity profile, and the blade geometry as discussed in ref. (11).

Due to swirl in the flow approaching the rotor, or from the use of non-radial upstream vanes, the wakes impinging on the rotor blades may have non-radial configuration. The wake-blade interaction in such cases does not occur simultaneously along the length of the blade and above Eq. (6) can be modified to account for such effects. Based on the analysis given by Filotas in ref. (12), the method of evaluating the fluctuating blade loads is developed in ref. (13) and one can write

$$\Delta L = \sum_{a=-\infty}^{\infty} (\Delta L)_a \hat{e}^{-i\phi_a} e^{-i(aV\Omega t - aV\psi_w)} \quad (7)$$

The angle ψ_w in the above equation, measured positive in the direction of rotor rotation, is the angle between the meridional planes containing the wake location at radius r and at hub.

In Rao Fan 2, upstream stators containing leaning vanes were employed, and the consequent values of ψ_w at the rotor plane are described in ref. (7). The influence of such oblique wake-blade interaction on the fundamental (i.e. $a = 1$) component of the fluctuating blade loading is evaluated in ref. (14) for various vane-lean angles employed in Rao Fan 2. Radial variation of amplitude and phase angle for radial vanes and leaning vane configuration 3, described in ref. (7), are presented in Figs. (6) and (7) respectively. The large radial variation of phase angle shown in Fig. (7) is essentially due to the variation of relative velocity at the rotor in Rao Fan 2.

Let us examine the events occurring in the elemental annulus $2\pi r dr$ under consideration. We have B number of blade elements, each experiencing load fluctuations as given by Eq. (7), but with a time delay of $\frac{1}{BN}$ between successive elements. Appropriate summation of events occurring on B number of blades crossing V number of wakes, as shown in ref. (14) would yield the following representation for the fluctuating force distribution on the elemental annulus.

$$dF = -\frac{B}{2\pi} \sum_{n=1}^{\infty} \sum_{a=-\infty}^{\infty} (\Delta L)_a e^{i(m\theta - \phi_{ma})} e^{-i(ka_0 t - aV\psi_w)} \quad (8)$$

where $ka_0 = 2\pi n BN$

n = harmonic index ($=1$ for blade passing frequency)

$m = nB - aV$, but takes on values between $-\infty$ and $+\infty$ (9)

Above Eq. (8) is similar to Eq. (4) derived earlier for the steady state loading on rotor blades. However, we observe that the n th harmonic of the above impressed force contains contributions from all the a th components of the fluctuating load on the rotor blades. Taking the axial and tangential components of the externally applied force described by Eq. (8) we obtain

$$dF_1 = dF \sin \lambda_r$$

$$\text{and } dF_3 = dF \cos \lambda_r$$

where λ_r = the rotor blade stagger angle. (10)

The acoustic radiation from the dipole sources equivalent to the fluctuating forces described above, can be examined using the second term of Eq. (1). It is shown in ref. (15) that the acoustic pressure at the field point (R, ψ) is then given by

$$\Delta p_n = \frac{-k_B}{4\pi R} e^{-ika_0(t-R/a_0)} \sum_{a=-\infty}^{\infty} \left\{ \left(\sin \lambda_r \cos \psi - \frac{m \cos \lambda_r}{kr} \right) (-i)^{m+1} \right. \\ \left. \times (\hat{A}_L)_a e^{i(aV\psi_w - \phi_{ma})} J_m(kr \sin \psi) \right\} \quad (11)$$

with the values of m given by

$$m = nB - aV.$$

Since the exponents of ψ_w and ϕ_{ma} depend upon radius r and the summation extends over several values of m and a , we shall abstain from expressing the rms value of pressure described above. The above equation agrees with the representation given by Lowson (16). Integrating right hand side of

Eq. (11) over $r_h \leq r \leq r_t$, we obtain the contribution to fan noise from the dipole sources due to wake-blade interaction forces. The results of such computations on Rao Fan 2 are given in ref. (14). The directivity of sound pressure level for the typical vane configurations is presented in Fig. (8). The contribution to fan noise from periodic blade loading is several orders of magnitude larger than that from steady state blade loading, shown in Fig. (4). This is a consequence of the Bessel functions of order m in Eq. (11) and NB in Eq. (5). The significance of wake-blade interaction in fan noise generation depends strongly on blade-vane number ratio. Even though the use of leaning vanes decreases sideline noise as indicated in Fig. (8) and confirmed in measurements reported in ref. (7), the periodic blade loading considered here is inadequate to predict fan noise at on-axis points.

The effect of inflow distortion on blade loading and resulting noise can be obtained by substituting $V = 1$ in Eq. (6), and the amplitude $(\Delta L)_a$ depends on Fourier series representing the distortion. Since inflow distortion is more diffused than the narrow wakes of stator vanes, as the index a increases the amplitude $(\Delta L)_a$ decreases rapidly. A double Fourier series in r and θ , to represent the flow distortion yields the corresponding value of $(\Delta L)_a$ as a function of radius.

Before closing the discussion on periodic fluctuations in blade loading, it is interesting to note the influence of the wakes from support struts in LF336 fan impinging upon the downstream

rotor blades. There is a major strut spanning the fan annulus and also a minor strut perpendicular to it. The noise generated by the presence of the minor strut can be ignored relative to that due to the major strut, as discussed in ref. (17). The major strut spanning the inlet can be considered as two radial vanes upstream of the rotor and one can employ Eq. (9) to evaluate the radiated acoustic field. In using Eq. (9) for acoustic computations on Rao Fan 2, it is found that a single value of $a = 1$ is sufficient. Higher values of a , and associated higher orders m of the Bessel function led to negligible changes in the computed results. However, in the case of LF336 fan with $B = 42$ and $V = 2$ (corresponding to one strut across the fan annulus), all values of a ranging from 1 to 21 had to be included and such computations were reported in ref. (17).

To illustrate the radial variation of the fluctuating loads on the rotor blades in LF336 caused by the major strut the amplitudes $(\hat{\Delta L})_a$ and phase angles ϕ_a are presented in Figs. (9) and (10) respectively for values of $a = 1$ and 21. To illustrate the dependence of each harmonic component of ΔL on the index a , the vector

$$(\Delta L)_a = (\hat{\Delta L})_a e^{-i\phi_a}$$

at the hub location of the blade for all the values of index a considered is shown in Fig. (11). The variation of the phase angle ϕ_a with the index a is primarily due to the frequency of the a th component of the fluctuations in the flow conditions met by the rotor blade as discussed in ref. (11).

Acoustic computations based on the influence of the major strut in LF336, are presented in Fig. (12). The estimated sound pressure level at the field point on fan axis is within reasonable agreement with measurements reported in ref. (8). However, these estimates of the effect of major strut fell far below the levels measured on the side line, indicating that radiation from other acoustic sources needs to be considered.

II.B.2. Random Fluctuations in Rotor Blade Load

The flow conditions experienced by a rotor blade element, due to turbulence in the inflow to the fan, may contain randomly fluctuating component v_0' . In the following we consider the random loading on the blades and acoustic radiation therefrom. Based on the discussion presented in ref. (18) the power spectrum of the turbulent fluctuations of v_{0n}' , component normal to blade chord, can be represented as

$$\Phi_{v_{0n}'}(\omega') = \frac{\ell}{v_0^2} \frac{1}{\pi v_0} \frac{1+3(\ell \omega'/v_0)^2}{\left\{1+(\ell \omega'/v_0)^2\right\}^2} \quad (12)$$

where v_0 = mean flow relative to blade
and ℓ = length scale of turbulence.

The fluctuating cross-component of velocity would give rise to fluctuating lift force on the blade. Based on an approximation suggested by Liepmann (19) for the lift response function, we can write the power spectrum of the fluctuating lift force per unit span of a blade as

$$\Phi_L(\omega') = (\pi \rho_0 v_0^2 c_r)^2 \frac{\Phi_{v_{0n}'} / v_0^2}{1 + \pi c_r \omega' / v_0} \quad (13)$$

where c_r = rotor blade chord

and Φ_{v_0} = the spectrum described in Eq. (12).

If the random fluctuation occurring on one blade element has no correlation with that on other elements on the blade and also with that on other blade elements in the fan annulus, the acoustic radiation from such random forces will give rise to broad band noise. However, if the length scale of the turbulence is such that an eddy is crossed by several blades before it loses its identity, we can observe sharp peaks in the noise spectrum at the blade passing frequency and its harmonics.

This number of possible crossings is given by

$$\beta_1 = \text{largest integer smaller than } BN \frac{\ell}{U_{01}} \quad (14)$$

where ℓ_1 = length scale (axial direction) for v_{0n} fluctuations.

and U_{01} = axial velocity considered here to be the same as the velocity with which the eddy is convected downstream.

Depending upon the length scale in the tangential direction, it is possible for more than one blade to experience the same conditions simultaneously. The number of such blades is given by

$$\beta_3 = \text{lowest integer larger than } \frac{\ell_3}{d} \quad (15)$$

where ℓ_3 = length scale (tangential direction) for v_{0n} fluctuations.

and d = blade spacing

To facilitate our computation, we made a simplifying assumption that the velocities occurring over a span length ℓ_2 (the

turbulence scale in the radial direction) are the same as those occurring at the center of the eddy.

Taking into account axial components of the random lift forces on all blade elements in the fan annulus from $r = r_h$ to r_t , it is shown in ref. (20) that the power spectrum of radiated acoustic pressure at field point (R, ψ) can be written as

$$\Phi_p(\omega) = \frac{B}{16\pi^2 R^2 a_0^2} \ell_2 \sum_{m=-\infty}^{\infty} \omega^2 \int_{r_h}^{r_t} f(\beta_1) f(\beta_3) \times \left\{ J_m^2 \left(\frac{\omega}{a_0} r \sin \psi \right) f^2(\lambda) \Phi_L(m\Omega - \omega) \right\} dr \quad (16)$$

$$\text{where } f(\beta_1) = \left\{ \frac{1 - \cos 2\pi \beta_1 \omega / B\Omega}{1 - \cos 2\pi \omega / B\Omega} \right\}$$

$$f(\beta_3) = \frac{1}{\beta_3} \left\{ \frac{1 - \cos 2\pi m \beta_3 / B}{1 - \cos 2\pi m / B} \right\} ; f(\lambda) = \sin \lambda \cos \psi - \frac{m a_0 \cos \lambda}{(\omega + m\Omega)r}$$

and $\Phi_L(m\Omega - \omega)$ = function described by Eq. (13) at $\omega' = (m\Omega - \omega)$.

Evaluation of the right hand side of above Eq. (16) becomes simple for axis points, since we set $\psi = 0$. The results of power spectrum of acoustic pressures thus computed on Rao Fan 2 and LF336 are presented in Figs. (13) and (14). These preliminary computations show the effect of increased length scale of turbulence as reported by Mani (21). The band width at blade passing frequency resulting from our computations on the axis appears to be narrower than that reported in ref. (21) for the total acoustic power from the fan. To illustrate the directivity

of discrete tone noise at the blade passing frequency, we evaluated the right hand side of above Eq. (16) at various aspect angles and the results for Rao Fan 2 are shown in Fig. (15).

II.C. Unsteady Loading on Outlet Guide Vanes

Since the locations of the stator vanes are stationary, only the unsteady loads on the vanes need be considered. These unsteady loads can originate from periodic interaction with wakes from upstream blades or from random velocity fluctuations in the turbulent regions.

II.C.1. Periodic Fluctuations in Vane Loading

Outlet guide vanes positioned downstream of a rotor are subjected to unsteady flow conditions due to periodic impingement of rotor wakes. As in our earlier discussions, let us direct our attention to an annulus $2\pi r dr$ containing V number of stator vanes downstream of B number of blades. The primary influence of the velocity deficit in each wake is to cause fluctuations in the incidence angle of mean flow on the vane element. Since a vane element is subjected to B number of wakes during each rotor revolution, these fluctuations will have a fundamental frequency BN , and the resulting fluctuating lift on the vane element can be expressed as the real part of the complex quantity

$$\Delta L = \sum_{n=1}^{\infty} (\Delta L)_n e^{-i\phi_n} e^{-inB\Omega t} \quad (17)$$

where the index $n = 1$ corresponds to the blade passing frequency. Above Eq. (17) is similar to Eq. (6) presented earlier for blade loading harmonics, except that the fundamental frequency here is B_N in place of V_N employed in Eq. (6).

Due to the swirl in the flow downstream of the rotor, and due to non-radial disposition of the blade trailing edge, the wakes from the rotor blade would occupy non-radial positions as they reach the stator plane. Consequently, wake impingement on a vane does not occur simultaneously along its length. To increase the obliquity of wake-vane interaction, the vanes in the downstream stator can be made to lean in the direction of rotor rotation. Modification of above Eq. (17) to take into account such oblique wake-vane interaction is discussed in ref. (15), and the fluctuating lift on the vane element can be described as

$$\Delta L = \sum_{n=1}^{\infty} (\Delta L)_n \hat{e}^{-i\phi_n} e^{-inB\Omega t} e^{-inB(\psi_w - \psi_v)} \quad (18)$$

The angles ψ_w and ψ_v in the above equation denote respectively the angular locations of the wake and the vane at radius r measured from the meridional plane containing the vane location at the hub. In the notation employed here both ψ_w and ψ_v are measured positive in the direction of rotor rotation. The method of evaluating the amplitude $(\Delta L)_n$ and phase angle ϕ_n of each n th harmonic component in above Eq. (18) is discussed in detail in ref. (13), and the obliquity of wake impingement

plays an important role in determining the fluctuating lift load on the vanes. When the outlet guide vanes are radial, we can set $\psi_v \equiv 0$ in Eq. (18) and obtain a representation similar to Eq. (7) derived earlier. The exponent containing ψ_w has opposite sign in Eq. (18) compared to earlier Eq. (7), since the rotating wakes impinge on stationary vanes in the present case.

Computations were carried out on the 45 radial vane configuration of LF336 for the amplitude and phase angle of the fundamental component ($n=1$) of the fluctuating load, represented by Eq. (18) above, and the results are presented in Figs. (5) and (16). As the rotor-stator gap is increased to twice the rotor chord length, the severity of wake-velocity deficit is reduced and the obliquity of wake impingement increases. The combined effect is that the magnitude of the fluctuating load on the vanes is considerably reduced. With the radial vanes we have $\psi_v \equiv 0$, but ψ_w increases with rotor-stator gap. Calculations on various OGV configurations on LF336 are presented in ref. (14).

Let us assume that all the vane elements within the elemental annulus $2\pi r dr$ are identical and the flow conditions in each of the rotor blade wakes are the same. Even though each vane element experiences lift fluctuations described by Eq. (18), the events on successive vanes occur with a time delay $\frac{1}{NV}$, which is the time taken by a wake to travel from one vane to the next. We can consider the force ΔL described by Eq. (18)

as concentrated at each vane location, but the fluctuations containing a delay term consistent with its location.

Acoustic radiation from an array of such concentrated forces (dipole sources) as described above is examined in ref. (15). The n th harmonic component of sound pressure at the field point (R, ψ) due to such sources in an elemental annulus $2\pi r dr$ is shown to be

$$\Delta p_n = \frac{ik e^{-ika_0(t-R/a_0)}}{4\pi R} (\Delta L)_n e^{-i\phi_n} \sum_{j=1}^V e^{ika_0 \tau_j} \left\{ (\sin \lambda_s \cos \psi - \cos \lambda_s \sin \theta_j \sin \psi) e^{-ikr \cos \theta_j \sin \psi} \right\} \quad (19)$$

where $\theta_j = 2\pi(j-1)/V$, and $\tau_j = \theta_j/2\pi N$

In the above equation, we observe that the various functions appearing on the right hand side depend upon the radial location of the sources considered. After summing over the V number of vanes and integrating from $r = r_h$ to r_t we can evaluate the rms value of acoustic pressure at the field point (R, ψ) . The results of such computations on LF336 operating at design conditions is presented in Fig. (17) as SPLdB at 150 ft. distance from fan center. By integrating the acoustic intensity over $\psi = 0$ to 180° , we obtain the total power of radiated sound. The power levels thus estimated, at the blade passing frequency are presented in ref. (14) and show good agreement with those calculated from measured data. However, the directivity of radiated acoustic field as presented in Fig. (17) is far different from the measurements reported in

ref. (8). Also, the ordered dipole sources arising from the wake-vane interaction considered here yield zero sound pressure along the fan axis. Consequently, it appears that the noise sources considered here, by themselves are insufficient to predict fan noise.

Before closing the discussion on periodic fluctuations in vane loading, it is interesting to note that the concentrated loads at the vane locations can be replaced by a continuous distribution with appropriate Fourier coefficients. Such representation was derived in ref. (22), and the wake-vane interaction effect is equivalent to the following force distribution exerted on the elemental annulus $2\pi r dr$ at the stator location.

$$dF = -\frac{V}{2\pi} \sum_{n=1}^{\infty} \sum_{m=-\infty}^{\infty} (\hat{\Delta L})_n \left\{ e^{i(m\theta - \phi_{mn})} e^{-i(ka_0 t + nB\psi_w)} \times e^{-i(m-nB)\psi_v} \right\} \quad (20)$$

where $ka_0 = 2\pi NBn$

$$m = nB - aV$$

and $a = \text{all integers from } -\infty \text{ to } +\infty \text{ including zero.}$

In terms of the index a , one can rewrite the above equation as

$$dF = -\frac{V}{2\pi} \sum_{n=1}^{\infty} \sum_{a=-\infty}^{\infty} (\hat{\Delta L})_n \left\{ e^{i(m\theta - \phi_{mn})} e^{-i(ka_0 t + nB\psi_w)} \times e^{iaV\psi_v} \right\} \quad (21)$$

and observe the similarity with previous Eq. (8) derived for force distribution in rotor plane. The axial and tangential components of the force described above are respectively

$$\begin{aligned} dF_1 &= dF \sin \lambda_s \\ \text{and } dF_3 &= -dF \cos \lambda_s \end{aligned} \quad (22)$$

where λ_s = outlet guide vane stagger angle

The tangential component here has a sign opposite to that of the corresponding term in Eq. (10), since the torque on the OGV stator is opposite to that on the rotor. Using these externally impressed forces in the second term of Eq. (1), the radiated acoustic field can be evaluated. As shown in ref. (22), the n th harmonic of the acoustic pressure at the field point contributed by the forces on elemental annulus $2\pi r dr$ of the stator plane can be written as

$$\Delta P_n = \frac{kV}{4\pi R} e^{-ika_0(t-r/a_0)} \sum_{a=-\infty}^{\infty} \left\{ (\sin \lambda_s \cos \psi + \frac{m}{kr} \cos \lambda_s)(-i)^{m+1} \right. \\ \left. \times (\hat{\Delta L})_n e^{-i(nB\psi_w + \phi_{mn})} e^{iaV\psi_v} J_m(kr \sin \psi) \right\} \quad (23)$$

where $m = nB - aV$.

One observes the similarity of this equation with Eq. (11) derived earlier for fluctuating loads on rotor blades. The term containing $\cos \lambda_s$ has a change in sign, because of the opposite sense of torque on the OGV stator relative to that on the rotor. The above equation agrees with the representation given by Lawson in ref. (16), except that the non-radial orientations of the wakes and the vanes are included here. Since

all the terms on the right hand side of Eq. (23) are dependent upon r , one completes the integration over r from $r = r_h$ to r_t before evaluating the rms value of the acoustic pressure at the field point. Typical computations were carried out on LF336 using above Eq. (23). The difference between the results obtained by using Eq. (23) and the earlier Eq. (19) is not discernible.

II.C.2. Random Fluctuations in Stator Vane Load

Each stator vane element experiencing turbulent velocity fluctuations, whether in the inflow or the wakes of upstream elements, would suffer random lift forces. However, since the vanes occupy fixed locations, the acoustic radiation from such random dipoles would have the same spectrum as the turbulence energy. Our present effort is in evaluating fan noise at the blade passing frequency and its harmonics. Hence, the investigation of the influence of turbulence on stator vanes is beyond the scope of this report.

III. QUADRUPOLE SOURCES IN AN AXIAL FAN

The influence of quadrupole sources can be examined from the first term on the right hand side of Eq. (1). By carrying out the differentiation with respect to x_i, x_j taking into account the retarded times, Lighthill (23) has shown that the pressure in the radiated field can be written as

$$p - p_o = \frac{1}{4\pi a_0^2} \int_V \sum_{i=1}^3 \sum_{j=1}^3 \frac{x_i x_j}{h^3} \left[\ddot{T}_{ij} \right] dv \quad (24)$$

The integration on the right hand side is to be carried out over the volume where \ddot{T}_{ij} is non-zero, and the square bracket indicates that the quantity is evaluated at retarded time.

As noted earlier, we can approximate

$$T_{ij} = \rho U_i U_j \quad (25)$$

where U is the velocity in the region with components $i, j = 1, 2, 3$. Before we can utilize the above Eqs. (24) and (25), we should examine the flow field in the fan annulus, i.e. obtain an appropriate description of velocity U . As mentioned earlier, the velocity field can be postulated in terms of the flow surrounding the blades, vanes or any other bodies immersed in the flow.

III.A. Description of Flow Field

Let us represent the velocity field as

$$U = U_o + U_{pr} + U_{ps} + U_{wr} + U_{ws} + v \quad (26)$$

where U_o denotes the steady state mean flow which may not

to be uniform in the fan annulus. The subscript p denotes the velocity field set up by the potential flow around the immersed bodies and the subscript w denotes that caused by the velocity deficit in the viscous wakes. The second subscript r or s refers to the contributions from rotor blades or stator vanes respectively. The last term v denotes random fluctuations of velocity.

For the sake of simplicity we shall ignore any distortion in the mean flow at the fan inlet. Also the random fluctuations v are thought of in terms of only the turbulent fluctuations and not those arising from blade-stall or other sources.

Each component, except v , in the above equation is well correlated i.e. the value at any one point is definable in terms of its value at any other point. On the other hand, the turbulent fluctuations v may have correlation only in a small region.

III.A.1. Steady State Mean Flow

Except in the region of the inlet bell-mouth, the radial component U_{02} can be ignored. The tangential component U_{03} is due to swirl behind the inlet guide vanes or behind the rotor in an OGV fan. Its magnitude will be much less than the axial component U_{01} .

III.A.2. Perturbations from Potential Flow

Let us consider an elemental annulus $2\pi r dr$ of the fan containing B number of blades or V number of vanes. The potential flow around these blade or vane elements can be obtained in terms of two-dimensional flow past a cascade of infinite number of airfoils. The cascade geometry and the uniform velocity through the cascade would be those corresponding to the conditions occurring at the annulus under consideration. Each airfoil in the cascade can be replaced by suitable distribution of vortices, sources and sinks to evaluate the flow field. Such analysis was presented in refs. (24) and (25). It is found that a description of the flow field upstream of the leading edges is simple. In between the leading and trailing edges abrupt changes in magnitude and phase angle occur. The perturbations from the mean flow are relatively small in the region downstream of the trailing edges.

Based on refs. (24) and (25) we can write the following expression for the axial component of the n th harmonic of velocity in the region upstream of rotor leading edge.

$$u_{pr,n} = \hat{u}_{pr,n} e^{i\phi_{pr,n}} e^{-2n\pi x'/d_r} e^{i(nB\theta - ka_0 t)} \quad (27)$$

where $\hat{u}_{pr,n}$ and $\phi_{pr,n}$ = the amplitude and phase angle of the component at blade leading edge

x' = distance measured upstream from rotor leading edge

and d_r = blade spacing.

The amplitude $\hat{U}_{pr_{in}}$ and the phase angle $\phi_{pr_{in}}$ depend upon the blade profile, blade loading, solidity and stagger angle. The above simple representation for $U_{pr_{in}}$ is applicable only upstream of leading edge since $\phi_{pr_{in}}$ does not depend upon x' in this region. Computations at pitch radius on Rao Fan 2 indicate that for the corresponding tangential component

$$\hat{U}_{pr_{in}} \approx \hat{U}_{pr_{in}}$$

and $\phi_{pr_{in}} = \frac{\pi}{2} + \phi_{pr_{in}}$

Consequently, we can write

$$U_{pr_{in}} \approx U_{pr_{in}} e^{i\pi/2} \quad (28)$$

Within the fan annulus the radial components will be relatively small and can be ignored in evaluating the quadrupole radiation.

In the case of a stator, the flow around the stationary vanes gives rise to velocity perturbations which are periodic in the circumferential direction. The fundamental period would be the vane spacing and the n th component of the perturbations related to the stator can be written as

$$U_{ps_{in}} = \hat{U}_{ps_{in}} e^{i\phi_{ps_{in}}} e^{-2n\pi x'/d_s} e^{in\theta} \quad (29)$$

$$U_{ps_{in}} \approx U_{ps_{in}} e^{i\pi/2} \quad (30)$$

where x' = distance measured from stator leading edge.

We observe the similarity between Eq. (27) derived earlier for the rotor related potential flow, and the above Eq. (29), since the only difference lies in translation of coordinate system with an angular velocity Ω . As in the case of rotor related flow field, here also we can ignore the components in the radial direction.

The method of evaluating flow perturbations arising from potential flow around the rotor blades and stator vanes, is discussed in detail in refs. (24) and (25). Non-radial orientation for rotor blades is seldom employed and Eq. (27) is suitable for all radial locations. We can substitute $\theta + \psi_v$ in place of θ in Eq. (29) to include the effect of non-radial vanes, with ψ_v described as a function of radius r .

III.A.3. Perturbations Due to Velocity Deficit in the Wakes
In the region downstream of stator vanes or support struts, there are present wakes with a velocity deficit relative to the mean flow through the fan annulus. The representation of flow downstream of a row of support struts is similar to that in the case of stator vanes, except that there are fewer number of wakes and the struts produce no swirl in the mean flow through the fan.

Let us consider an annular region $2\pi r dr$ downstream of a row of V number of stator vanes. This region will contain V number of wakes equally spaced along the circumference. The circumferential location of each wake at the annulus under

consideration will not be the same as that of the corresponding vane element in the stator, if there is any swirl present in the mean flow through the annulus. Let ψ_w^s , measured from a reference meridional plane, denote such circumferential location of a wake at the annulus under consideration. Let $(\delta v)^0$ denote the velocity defect at the wake center line and Y denote the wake half width. Both $(\delta v)^0$ and Y can be estimated from the vane section characteristics, mean flow velocity v_o at the stator, and the downstream distance from the stator. One can assume that across each wake there exists a velocity profile similar to that occurring in the wake of an isolated airfoil section. It is shown in ref. (11) that the integrated effect of N number of such wake can be represented by the real part of a complex Fourier series

$$(\delta v)_s = \sum_{a=1}^{\infty} 2(\delta v)_s^0 \frac{\sqrt{\pi}}{K_s} e^{iav(\theta - \psi_w^s)} e^{-(a\pi/K_s)^2} \quad (31)$$

$$\text{where } K_s = \frac{\sqrt{\pi}d_s}{Y} \cos \nu_s$$

d_s = circumferential spacing of the wakes, same as that of the stator vanes

ν_s = angle between the wake center line and normal to the elemental annulus

We observe that $(\delta v)_s^0$ on the right hand side of the above equation is measured in the same direction as the velocity v_o . Hence, the components of the velocity perturbations caused by stator wakes can be written as

$$\begin{aligned}
 U_{ws_1} &= (\delta V)_s \cos \nu_s \\
 U_{ws_3} &= (\delta V)_s \sin \nu_s
 \end{aligned} \tag{32}$$

From equations (31) and (32) we observe that these velocity components depend upon the axial, radial and circumferential locations of the point, where they are to be evaluated. Since we have ignored radial components in our analysis, we can set

$$U_{ws_2} \equiv 0.$$

The analysis of flow field downstream of B number of blades will be similar to the above, if we consider the coordinate system attached to the rotor. However, in fixed coordinate system we obtain

$$(\delta V)_r = \sum_{n=1}^{\infty} 2(\delta V)_r^0 \frac{\sqrt{\pi}}{K_r} e^{inB(\theta - \psi_w^r)} e^{-(n\pi/K_r)^2} e^{-ika_0 t} \tag{33}$$

$$\text{where } ka_0 = 2\pi n B N$$

$$K_r = \frac{\sqrt{\pi} d_r}{Y} \cos \nu_r$$

d_r = circumferential spacing of the wakes, same as that of the rotor blades

ν_r = angle between the wake center line (in relative flow) and normal to the elemental annulus

Similar to Eq. (32), the velocity perturbations caused by rotor wake can be written as

$$\begin{aligned}
 U_{wr_1} &= (\delta V)_r \cos \nu_r \\
 U_{wr_2} &= 0 \\
 U_{wr_3} &= (\delta V)_r \sin \nu_r
 \end{aligned} \tag{34}$$

with $(\delta V)_r$ as defined by above Eq. (33). We observe that the index $n = 1$ corresponds to blade passing frequency.

In our analysis here, both θ and ψ_w are considered positive when measured in the direction of rotor rotation. The equations derived in this section are for velocity perturbations at any given point (r, θ, x) in the fan annulus and as such the respective parameters at the location should be used.

III.A.4. Random Velocity Fluctuations in Turbulent Regions

The velocity perturbations discussed in previous subsections 2 and 3 are well-ordered in the sense that the velocity at one point of the flow region has a definite space-time relation with the velocity at another point of the flow region. Any complete description of flow field cannot preclude the presence of random turbulent fluctuations. These random fluctuations can be present in the flow entering the fan, and also can be generated by various elements of the fan such as struts, rotor blades, stator vanes. Because of their very nature, we can only refer to these random fluctuations in terms of statistical quantities such as mean square values, probability density functions, correlation functions and power spectral density functions. In the study of fan noise problems, another important quantity is the correlation length, ℓ , which is defined as the area under the non-dimensional correlation function and thus represents some average size of the eddy within which two points in the flow field will have velocity fluctuations that can be considered as coherent or related.

The spectral distribution and the correlation length are not independent of each other. This is obvious for the reason that if low frequency fluctuations are dominant, the extent to which two points in the flow field are related will be larger. The way they are related depends on the particular model chosen to describe the turbulent field, as discussed in Appendix II of ref. (18).

For inlet turbulence, the assumption of homogeneity and isotropy is usually made. In other words, the mean square values of the fluctuating velocities do not depend on spacial location nor the coordinate system chosen. If a "frozen pattern" convected with velocity U_C is chosen, as discussed in Ref. (19), the spectra of the velocity components can be written in terms of longitudinal correlation length scale ℓ and mean square value $\overline{v_0^2}$ of the inlet turbulence

$$\Phi_{v_{01}}(\omega) = \frac{\overline{v_0^2}}{\pi} \frac{\ell}{U_C} \frac{1}{1 + \left(\frac{\omega\ell}{U_C}\right)^2} \quad (35)$$

and

$$\Phi_{v_{02}}(\omega) = \frac{\overline{v_0^2}}{\pi} \frac{\ell}{U_C} \frac{\frac{1+3\left(\frac{\omega\ell}{U_C}\right)^2}{\left\{1+\left(\frac{\omega\ell}{U_C}\right)^2\right\}^2}}{\left\{1+\left(\frac{\omega\ell}{U_C}\right)^2\right\}^2}, \text{ for positive values of } \omega \quad (36)$$

We note that $\overline{v_{01}^2} = \overline{v_{02}^2}$ for isotropic turbulence. The above spectral density functions are derived from an assumed exponential form for the longitudinal space correlation, and these were used in the dipole calculation. However for the quadrupole calculations, the space-time correlation function of the turbulent field is required. Based on the same model used before, it has been found that the space-time correlation for

the longitudinal velocity component is too complicated for the quadrupole evaluation. Thus a slightly different model has to be adopted. Without assuming isotropy, the space-time correlation function of the "frozen pattern" connected with velocity

U_C in the 1-direction can be written as

$$R(\xi, \tau) = \frac{1}{v_1^2} e^{-\left| \frac{\xi_1 - U_C \tau}{\ell_1} \right|} - \left| \frac{\xi_2}{\ell_2} \right| - \left| \frac{\xi_3}{\ell_3} \right| \quad (37)$$

where ξ is the separation vector with components ξ_1 , ξ_2 and ξ_3 .

If one is interested in that part of the noise generated by the true temporal fluctuation of the turbulent field, an additional time function has to be incorporated as explained in ref. (18).

For wake turbulence behind struts, blades or vanes, some phenomenological approach can be used to estimate the intensity level in terms of the mean flow and some properties of the airfoil. Ref. (26) shows that the root-mean-square value of turbulence can be written as

$$\tilde{v} = 0.2 (\delta v)^0 \quad (38)$$

and the length scale can be assumed as the mixing length leading to

$$\ell = 0.2Y \quad (39)$$

The velocity deficit $(\delta v)^0$ at wake center and wake half-width Y are discussed in the preceding subsection.

III.B. Ordered Quadrupoles Due to Periodic Velocity Fluctuations

Let us examine the consequence of the periodic components of the velocity fluctuations described in the preceding section. These velocity fluctuations are well ordered, i.e. the fluctuations at any two different points in the flow region have a definite phase relationship between them. Let us consider a point (r, θ, ξ) in the fan annulus and an elemental volume $rdr d\theta d\xi$ within which the velocities can be assumed to be the same as at the point considered. Restricting our attention only to the axial components of the fundamental of the periodic fluctuations of velocity, we substitute

$$U = U_o + U_{pr_{1(1)}} + U_{ps_{1(1)}} + U_{wr_{1(1)}} + U_{ws_{1(1)}} \quad (40)$$

into the right hand side of Eq. (24). The second subscript (1) in the above equation indicates the fundamental of the spatial or temporal perturbations. From the fundamental components of the velocity fluctuations, we can evaluate acoustic radiation at the blade passing frequency. The analysis can be easily extended to higher harmonics.

III.B.1. The Effect of Rotor Related Flow Field

In the region upstream of the rotor we have the velocity fluctuations U_{pr_1} , and in the downstream region we have the velocity fluctuations U_{wr_1} . From Eq. (27) we can write the following expression

$$U_{pr_{1(i)}} = \hat{U}_{pr_{1(i)}} \cos(B\theta - ka_0 t) \quad (41)$$

with $\hat{U}_{pr_{1(i)}} = \left\{ \hat{U}_{pr_{1(i)}} \right\}_{l.e.} e^{-2\pi x' / d_r}$

where x' = upstream distance from blade leading edge, and the subscript $l.e.$ denotes the amplitude at the blade leading edge.

Up to a downstream axial distance of two chord lengths velocity fluctuations caused by the wake and described in Eqs. (33) and (34) can be approximated as

$$U_{wr_{1(i)}} = \hat{U}_{wr_{1(i)}} \cos(B\theta - ka_0 t) \quad (42)$$

where the amplitude

$$\hat{U}_{wr_{1(i)}} = 4.84 \sigma_r v_0 \frac{c_{Dr}}{0.6 + \frac{2x''}{c_r \cos \nu_r}} \left\{ 0.15 + \frac{x''}{c_r \cos \nu_r} \right\}^{\frac{1}{2}}$$

with x'' = downstream axial distance from blade trailing edge and v_0 = velocity relative to rotor blades.

Acoustic pressure due to radiation from the "ordered" quadrupoles in the upstream region of the blades can be written as

$$p_{(i)} - p_0 = \frac{1}{4\pi a_0^2 R} \iint \int_{r_h}^{r_t} \int_{0}^{2\pi} \int_{-\infty}^{\infty} \cos^2 \psi \left[\frac{\partial^2}{\partial t^2} \left\{ 2\rho U_{(i)} U_{pr_{1(i)}} \right\} \right] r dr d\theta dx' \quad (43)$$

where $U_{pr_{1(i)}}$ is described by Eq. (41) and the square bracket indicates that the function is evaluated at retarded time. Completing the integration over θ we obtain the rms value of the contribution from the elemental annulus $2\pi r dr$ extending from $x' = 0$ to ∞ as

$$\widetilde{\Delta P}_{(1)} = \frac{k^2}{R\sqrt{2}} \rho U_{\infty} \cos^2 \psi J_B(kr \sin \psi) r dr \int_0^\infty \hat{U}_{pr_{(1)}} dx' \quad (44)$$

where $\hat{U}_{pr_{(1)}}$ is defined as a function of x' by Eq. (41).

Similarly the acoustic pressure due to radiation from the 'ordered' quadrupoles in the downstream region of the rotor can be written as

$$p_{(1)} - p_0 = \frac{1}{4\pi a_0^2 R} \int_{r_h}^{r_t} \int_0^{2\pi} \int_0^{2c_r} \cos^2 \psi \left[\frac{\partial^2}{\partial t^2} \left\{ 2\rho U_{\infty} U_{wr_{(1)}} \right\} \right] r dr d\theta dx'' \quad (45)$$

where $U_{wr_{(1)}}$ is described by Eq. (42).

The rms value of the contribution from the elemental annulus $2\pi r dr$ extending from $x'' = 0$ to $2c_r$ can be written as

$$\widetilde{\Delta P}_{(1)} = \frac{k^2}{R\sqrt{2}} \rho U_{\infty} \cos^2 \psi J_B(kr \sin \psi) r dr \int_0^{2c_r} \hat{U}_{wr_{(1)}} dx'' \quad (46)$$

let us consider only the axial component of the steady state blade loading and rewrite Eq. (5) as

$$\widetilde{\Delta P}_{(1)} = \frac{kB}{2\pi R\sqrt{2}} \Delta L \sin \lambda_r \cos \psi J_B(kr \sin \psi) \quad (47)$$

We observe certain amount of similarity in the expressions given in Eqs. (44), (46) and (47) for the contributions from the various sources. For example, comparing Eq. (44) with Eq. (47) we can write

$$\frac{\tilde{\Delta p}_{(1)} \text{ from Eq. (44)}}{\tilde{\Delta p}_{(1)} \text{ from Eq. (47)}} = \frac{k\rho U_{O_1} \cos \psi}{B \Delta L \sin \lambda_r} 2\pi r dr \int_0^\infty \hat{U}_{pr_{(1)}} dx' \quad (48)$$

Since $\Delta L \sin \lambda_r$ is the axial force per blade element in the annulus under consideration, let us define a thrust coefficient C_T by the equation

$$\Delta L \sin \lambda_r = \frac{\rho}{2} V_0^2 C_T c_r dr \quad (49)$$

The total strength of quadrupoles present in the volume considered divided by the number of blades gives us quadrupole strength per blade and let us define a coefficient C_Q by the following equation.

$$\frac{\rho}{2} V_0^2 c_r^2 dr C_{Q_{(44)}} = \frac{2\pi}{B} r dr \rho V_0 \int_0^\infty \hat{U}_{pr_{(1)}} dx' \quad (50)$$

Subscript (44) on C_Q denotes that the evaluation is in terms of quadrupoles employed in deriving Eq. (44).

Substituting Eqs. (49) and (50) into Eq. (48) we obtain

$$\frac{\tilde{\Delta p}_{(1)} \text{ from Eq. (44)}}{\tilde{\Delta p}_{(1)} \text{ from Eq. (47)}} = B M_t \frac{c_r}{r} \cos \psi \frac{C_{Q_{(44)}}}{C_T} \frac{U_{O_1}}{V_0} \quad (51)$$

The comparison made above was also observed by Ffowcs Williams and Hawking (4). The importance of the ordered quadrupoles increases with the number of blades and the tangential velocity of the blades. By comparing Eq. (46) with Eq. (44) we can write

$$\frac{\tilde{\Delta p}_{(1)} \text{ from Eq. (46)}}{\tilde{\Delta p}_{(1)} \text{ from Eq. (44)}} = \frac{\int_0^\infty U_{wr_{(1)}} dx''}{\int_0^\infty U_{pr_{(1)}} dx'} \simeq 3l C_{D_r} \sigma_r^2 \quad (52)$$

Considering the magnitude of blade section drag coefficient, we can conclude that "ordered" quadrupoles present in the region downstream of a rotor are of the same importance as those present in the upstream region.

III.B.2. Effect of Stator Related Flow Field

The presence of stator vanes give rise to perturbations to the mean flow through the fan. As discussed in an earlier subsection, these perturbations have space-wise dependence, but are of steady state nature. Consequently, the stator related flow perturbations in themselves produce no noise. However, the presence of periodic fluctuations due to rotor flow field coupled with the space-wise perturbations due to stator can generate noise at the blade passing frequency and its harmonics.

Let us examine the case of outlet guide vanes for example. Using the analyses developed in the preceding section, in the region upstream of the stator the fundamental component of axial velocity perturbations can be written as

$$U_{ps_{1(1)}} = \hat{U}_{ps_{1(1)}} \cos V\theta \quad (53)$$

where V = number of outlet guide vanes, and

$$\hat{U}_{ps_{1(1)}} = \left\{ \hat{U}_{ps_{1(1)}} \right\}_{l.e.} e^{-2\pi x'/d_s}$$

and x' = upstream axial distance from stator leading edge.

In the region downstream of the stator up to two chords length, the axial component of the fundamental of the perturbations can be approximated by

$$U_{ws_{1(1)}} = \hat{U}_{ws_{1(1)}} \cos \nu \theta \quad (54)$$

where

$$\hat{U}_{ws_{1(1)}} = 4.84 \sigma_s V_o \frac{C_{D_s}}{0.6 + \frac{2x''}{C_s \cos \nu_s}} \left\{ 0.15 + \frac{x''}{C_s \cos \nu_s} \right\}^{\frac{1}{2}}$$

V_o = velocity relative to stator vanes

and x''_s = downstream distance from stator trailing edge.

The fundamental of the axial velocity fluctuations caused by the rotor wake are already described earlier in Eq. (42). In the region of interest say one chord upstream and two chord downstream of the stator, let us assume the amplitude $\hat{U}_{wr_{1(1)}}$ in Eq. (42) to be constant and equal to its value at the stator midchord station. Such an approximation would yield higher estimates but is convenient for comparison with the corresponding "ordered" dipole radiation from periodic fluctuating forces on the outlet guide vanes discussed in section II.C.1.

Considering the radiation from the "ordered" quadrupoles in the region upstream of the stator, we can write the rms value of acoustic pressure as

$$\tilde{\Delta p}_{(1)} = \frac{k^2}{R\sqrt{2}} \rho \hat{U}_{wr_{1(1)}} \cos^2 \psi J_{B-V}(kr \sin \psi) r dr \int_0^\infty \hat{U}_{ps_{1(1)}} dx' \quad (55)$$

Similarly from the region downstream of the stator we can write

$$\tilde{\Delta p}_{(1)} = \frac{k^2}{R\sqrt{2}} \rho \hat{U}_{wr_{1(1)}} \cos^2 \psi J_{B-V}(kr \sin \psi) r dr \int_0^{2C_s} \hat{U}_{ws_{1(1)}} dx'' \quad (56)$$

From Eq. (23) describing the acoustic radiation from "ordered" dipoles on the outlet guide vanes due to rotor wake impingement,

we can restrict our attention to only the fundamental of the axial component of the fluctuating load, and write

$$\widehat{\Delta P}_{(1)} = \frac{KV}{4\pi R\sqrt{2}} (\widehat{\Delta L})_{(1)} \sin \lambda_s \cos \psi J_{B-V}(kr \sin \psi) \quad (57)$$

where $(\widehat{\Delta L})_{(1)}$ is the amplitude of the fundamental of fluctuating lift force on the vane element in the annulus $2\pi r dr$ due to periodic impingement by the rotor wakes.

The magnitude of $(\widehat{\Delta L})_{(1)}$ depends upon the amplitude of the fundamental of the upwash (component normal to v_o) fluctuations experienced by the vane element, which can be approximated by

$$\frac{\sin(\nu_r + \nu_s)}{\cos \nu_r} \widehat{U}_{wr_{(1)}}$$

and the lift transfer function discussed by Kemp and Sears in ref. (11).

Using the value suggested in ref. (19) for the lift transfer function we can write

$$(\widehat{\Delta L})_{(1)} = \pi \rho v_o \widehat{U}_{wr_{(1)}} c_s dr \frac{\sin(\nu_r + \nu_s)}{\cos \nu_s} \left\{ 1 + \frac{\pi k a_0 c_s}{v_o} \right\}^{-\frac{1}{2}} \quad (58)$$

Let us compare the contribution from the ordered quadrupoles considered in Eq. (55) with that from the ordered dipoles as given by Eq. (57). Substituting Eq. (58) into (57) we can obtain the ratio

$$\frac{\tilde{\Delta P}_{(1)} \text{ from Eq. (55)}}{\tilde{\Delta P}_{(1)} \text{ from Eq. (57)}} = 4 \frac{k}{V} \frac{r}{c_s} \cos \psi \frac{\cos \nu_s}{\sin \lambda_s \sin(\nu_r + \nu_s)} \times \left\{ 1 + \frac{\pi k a_0 c_s}{V_o} \right\}^{\frac{1}{2}} \int_0^{\infty} \frac{\hat{U}_{ps_{(1)}}}{V_o} dx' \quad (59)$$

Let us assume $\hat{U}_{ps_{(1)}}$ at the leading edge of the stator to be approximately equal to $0.4V_o$ and obtain

$$\int_0^{\infty} \frac{\hat{U}_{ps_{(1)}}}{V_o} dx' = 0.4 \frac{d_s}{2\pi}$$

We can also use simplifying approximations such as

$$(\nu_r + \nu_s) \approx \pi/2$$

$$\frac{\cos \nu_s}{\sin \lambda_s} \approx \frac{1}{\tan \nu_s} = \frac{U_{O_1}}{U_{O_3}}$$

For conditions usually met in lifting fans we can write

$$\left\{ 1 + \pi \frac{k a_0 c_s}{V_o} \right\}^{\frac{1}{2}} \approx 2\pi$$

Substituting the above approximations into Eq. (59) we obtain the ratio

$$\frac{\tilde{\Delta P}_{(1)} \text{ from Eq. (55)}}{\tilde{\Delta P}_{(1)} \text{ from Eq. (57)}} = 1.6 \frac{B}{V} M_t \sigma_s \cos \psi \frac{U_{O_1}}{U_{O_3}} \quad (60)$$

and observe that the contribution from the quadrupoles considered here is of the same order of magnitude as that from the periodic forces on the vanes due to impingement by rotor wakes.

By comparing the contributions from the ordered quadrupoles in the downstream and upstream region of the stator as given by Eqs. (56) and (55) respectively, we obtain a ratio similar to that derived in earlier Eq. (52). Consequently, we can conclude that the ordered quadrupoles in these two regions are of equal importance in evaluating fan noise.

III.C. Random Quadrupoles Due to Inflow Turbulence

In the preceding subsection we have discussed the acoustic radiation from only the velocity fluctuations which are periodic. Since velocity fluctuations can also contain a random component due to turbulence, one should consider the resulting random quadrupole noise sources. For the present let us restrict our attention to the turbulent fluctuation in the inflow to the fan. The random fluctuations by themselves give rise to a broad band noise, whose magnitude is governed by the intensity and power spectrum of the inflow turbulence. However, the presence of the periodic component related to the rotor flow field can give rise to noise at blade passing frequency and its harmonics.

III.C.1. Effect of Rotor Potential Flow Field

In the upstream region of the rotor, we have periodic velocity fluctuations arising from potential flow around the blades, as described in subsection III.A.2, and random velocity velocity fluctuations whose power spectrum is discussed in subsection III.A.4. Let us consider a point (r, θ, ξ) in the fan annulus

and an elemental volume $rdrd\theta d\xi$ within which the velocity can be considered to be the same as at the point. Let us restrict our attention to the axial components of velocity perturbation and substitute

$$U = U_{pr_1} + v_0,$$

into Eq. (25) to define the elemental quadrupole strength. Considering the power spectrum

$$\Phi(\pm\omega) = \tilde{v}_0^2 \frac{\ell}{\pi U_c} \frac{1}{1 + \left(\frac{\omega\ell}{U_c}\right)^2}$$

for the turbulent fluctuations, and the sinusoidal nature

$$U_{pr_{1(i)}} = \hat{U}_{pr_{1(i)}} \cos B\Omega t$$

of the rotor related component at the blade passing frequency we can show that the power spectrum of the elemental quadrupole source is

$$\begin{aligned} \Phi_Q(\pm\omega) = & \left\{ 2\rho \hat{U}_{pr_{1(i)}} \right\}^2 \tilde{v}_0^2 \frac{\ell}{\pi U_c} \left\{ \frac{1}{1 + \left\{ \frac{B\Omega\ell}{U_c} - \frac{\omega\ell}{U_c} \right\}^2} \right. \\ & \left. + \frac{1}{1 + \left\{ \frac{B\Omega\ell}{U_c} + \frac{\omega\ell}{U_c} \right\}^2} \right\} \end{aligned} \quad (61)$$

The convection velocity U_c of the "frozen convective pattern" model of turbulence employed in the above equation can be approximated by the mean axial velocity U_{o_1} . Let us consider an eddy size of dimensions ℓ_1 , ℓ_2 and ℓ_3 along the axial,

radial and circumferential directions respectively. For isotropic turbulence we have $\ell_1 = 2\ell_2 = 2\ell_3 = \ell$. A simplifying assumption would be that the turbulent fluctuations are perfectly correlated within the eddy volume and uncorrelated with fluctuations elsewhere. However, the rotor related sinusoidal fluctuations give rise to different retarded times for radiation from different portions of the eddy. Acoustic radiation from such quadrupole sources was discussed in ref. (20). The mean square pressure at the field point due to sources with an annulus $2\pi r dr$ extending from rotor leading edge to infinite distance upstream can be written as

$$\Delta \bar{p}_1^2 = \frac{\cos^4 \Psi}{32\pi a_0^2 R^2} (ka_0)^4 \ell_1 \ell_2 \ell_3 \Phi_Q(B\Omega) f_1 f_3 2\pi r dr \frac{\pi U_0}{\ell_1}$$

$$\text{where } f_1 = \left\{ \frac{d}{2\pi \ell_1} \right\}^2 \left\{ \int_0^{\frac{\pi}{2} \ell_1} \left\{ e^{-n\pi(2x^1 + \ell_1)/d} - 1 \right\}^2 dx^1 + \int_{\frac{\pi}{2} \ell_1}^{\infty} e^{-4\pi x^1/d} \left\{ e^{\pi \ell_1/d} - e^{-\pi \ell_1/d} \right\}^2 dx^1 \right\}$$

$$f_3 = \left\{ \frac{d}{\pi \ell_3} \sin \frac{\pi \ell_3}{d} \right\}^2$$

and $\Phi_Q(B\Omega)$ = the right hand side of Eq. (61) at $\omega = B\Omega$

By integrating above equation from $r = r_h$ to r_t one can evaluate the acoustic radiation from longitudinal-axial quadrupole sources in the fan annulus upstream of the rotor. Results of such computations on Rao Fan 2 at 5 ft. distance on axis are presented in Fig. (17) for various values of length scale ℓ .

III.C.2. Effect of Rotor Wakes

Downstream of the rotor blades, we have periodic fluctuations in velocity as discussed in section III.A.3. Similar to the analysis presented in the preceding subsection, let us examine the effect of the axial component of the fundamental of such velocity fluctuations. Up to an axial downstream distance of twice the rotor chord, the axial component of the fundamental of velocity fluctuations have already been described by Eq. (42). The periodic component of the velocity fluctuations considered in the preceding section are those described by Eq. (41). We recognize the similarity between these two equations and the acoustic radiation from the random quadrupole source in this region can be approximated by comparing the integral

$$\int_0^{\infty} \left\{ \frac{\hat{U}_{pr}^{(1)}}{V_o} \right\}^2 dx' \simeq 0.16 \frac{d_r}{4\pi} \quad (63)$$

with the integral

$$\int_0^{2c_r} \left\{ \frac{\hat{U}_{wr}^{(1)}}{V_o} \right\}^2 dx'' \simeq 2.76 (C_{D_r} \sigma_r)^2 c_r \quad (64)$$

where V_o is the velocity relative to the rotor blades.

We note that the ratio of the above two integrals is approximately unity when we consider the values of C_{D_r} and σ_r usually occurring in axial fans. Consequently, we can estimate

that the noise radiated from the random quadrupole sources present in this downstream region is of the same order of magnitude as that discussed in the preceding subsection.

III.C.3. Effect of Stator Flow Field

The perturbations in flow field caused by the presence of stator vanes are of a steady-state type even though they depend upon spatial location. Consequently, the effect of random fluctuations associated with turbulence will give rise to quadrupole radiation having the same spectral distribution as the turbulence component. Our attention presently being the noise at blade passage frequency and its harmonics, consideration of the effects referred above are beyond the scope of this report.

III.D. Random Quadrupoles Due to Turbulence in the Wake Regions

In addition to the homogeneous turbulence present in the inflow to the fan, we have random turbulent fluctuation of velocity in the wake regions of the various elements of the fan. Even though the intensity of turbulence in these regions is greater than that in the inflow it is present only in a small portion of the fan annulus. Because of the rotor related periodic fluctuations, the associated quadrupoles can generate noise at blade passage frequency and its higher harmonics. Evaluation of acoustic radiation from the wake regions will be included in our future investigations.

IV. CONCLUDING REMARKS

This interim report describes the analytical methods employed along with some preliminary results obtained in our effort of evaluating noise sources in axial fans. Since acoustic measurements on fans show prominent peaks at blade passing frequency and its harmonics; we directed our attention to the discrete frequency noise. The information presented in this report is a step towards identifying predominant noise sources in a fan, and must be regarded as far from a complete understanding of the fan noise problem. However, based on the representative results given in this report the following conclusions can be reached.

- (1) The effect of steady-state blade loading can be ignored in estimating noise from fans with multi-bladed rotors.
- (2) The periodically fluctuating forces on rotor blades or stator vanes arising from wake-impingement can be a dominant noise source depending upon the blade-vane ratio. The noise level as well as its directivity can be altered by changing the number of stator vanes.
- (3) Quadrupole radiation from periodic fluctuations of axial velocity components in rotor-stator interaction can be of the same order of magnitude as the

dipole radiation from the periodic fluctuating loads on blades or vanes caused by wake impingement.

- (4) Inherent cancellation of acoustic radiation from "ordered" sources distributed in the fan annulus yields zero noise along fan axis.
- (5) Turbulence present in the inflow to the fan can be an important contributor to discrete frequency noise because of the random forces on the rotor blades. Acoustic radiation from random quadrupoles is relatively unimportant.

As mentioned earlier, further effort on several items briefly mentioned in this report is necessary for a complete understanding of acoustic radiation from axial fans and to be able to arrive at design features to reduce noise.

REFERENCES

1. Lighthill, M. J., "Sound Generated Aerodynamically" The Bakerian Lecture, Proceedings of the Royal Society of London, Vol. 276, Series A, 1962, pp. 147-186.
2. Curle, S. N., "The Influence of Solid Boundaries Upon Aerodynamic Sound", Proc. of the Royal Society Series A, Vol. 231, pp. 505-514, 1955.
3. Richards, E. J. and Mead, D. J., Noise and Acoustic Fatigue in Aeronautics, John Wiley & Sons, Ltd., New York, 1968.
4. Ffowcs Williams, J. E. and Hawkins, D. L., "Theory Relating to the Noise of Rotating Machinery", Aeronautical Research Council, London, Eng., ARC 29.821, Jan. 1968.
5. Tyler, J. M. and Sofrin, T. G., "Axial Flow Compressor Noise Studies", Trans. of the Soc. of Automotive Engineers, 1961.
6. Monthly Progress Report No. 4 on "Analytical Lift Fan Noise Study", Contr. No. NAS2-6401, August 17, 1971.
7. Rao, G. V. R., "Study of Non-radial Stators for Noise Reduction", NASA CR-1882, September 1971.
8. "LF336/C Modification and Acoustic Test Program Data Report, Vol. 1", Sept. 1970. (prepared by General Electric Co.)
9. Gutin, L., "On the Sound Field of a Rotating Propeller", NACA TM 1195, October, 1948.
10. Filleul, N. LeS., "An Investigation of Axial Flow Fan Noise", J. Sound Vib., 1966, 3(2), pp 147-165.

11. Kemp, N. H. and Sears, W. R., "The Unsteady Forces Due to Viscous Wakes in Turbomachines", *Journal of the Aerospace Sciences*, Vol. 19, 1952, p. 713.
12. Filotas, L. T., "Response of an Infinite Wing to an Oblique Sinusoidal Gust: A Generalization of Sears' Problem", NASA SP-207, pp 231-246, Conference held at NASA Headquarters, Washington, D. C., July 14-15, 1969.
13. Monthly Progress Report No. 1 on "Analytical Lift Fan Noise Study", Contr. No. NAS2-6401, May 7, 1971.
14. Monthly Progress Report No. 5 on "Analytical Lift Fan Noise Study", Contr. No. NAS2-6401, Sept. 1971.
15. Monthly Progress Report No. 2 on "Analytical Lift Fan Noise Study", Contr. No. NAS2-6401, June 10, 1971.
16. Lawson, M. V., "Theoretical Studies of Compressor Noise", NASA CR-1287, March 1969.
17. Monthly Progress Report No. 7 on "Analytical Lift Fan Noise Study", Contr. No. NAS2-6401, Nov. 8, 1971.
18. Monthly Progress Report No. 14 on "Analytical Lift Fan Noise Study", Contr. No. NAS2-6401, June 19, 1972.
19. Liepmann, N. W., "On the Application of Statistical Concepts to the Buffeting Problem", *Journal of the Aerospace Sciences*, Vol. 19, 1952, pp. 193-800.
20. Monthly Progress Report No. 13 on "Analytical Lift Fan Noise Study", Contr. No. NAS2-6401, May 11, 1972.
21. Mani, R., "Noise Due to Interaction of Inlet Turbulence with Isolated Stators and Rotors", *Journal of Sound Vib.* 17(2) 1971, pp. 123-132.
22. Monthly Progress Report No. 3 on "Analytical Lift Fan Noise Study", Contr. No. NAS2-6401, July 9, 1971.

23. Lighthill, M. J., "On Sound Generated Aerodynamically", Proceedings of the Royal Society of London, A211, pp. 564-587, 1952.
24. Monthly Progress Report No. 11 on "Analytical Lift Fan Noise Study", Contr. No. NAS2-6401, March 7, 1972.
25. Monthly Progress Report No. 12 on "Analytical Lift Fan Noise Study", Contr. No. NAS2-6401, April 19, 1972.
26. Abramovich, G. N., "The Theory of Turbulent Jets", The M.I.T. Press, Massachusetts, 1963.

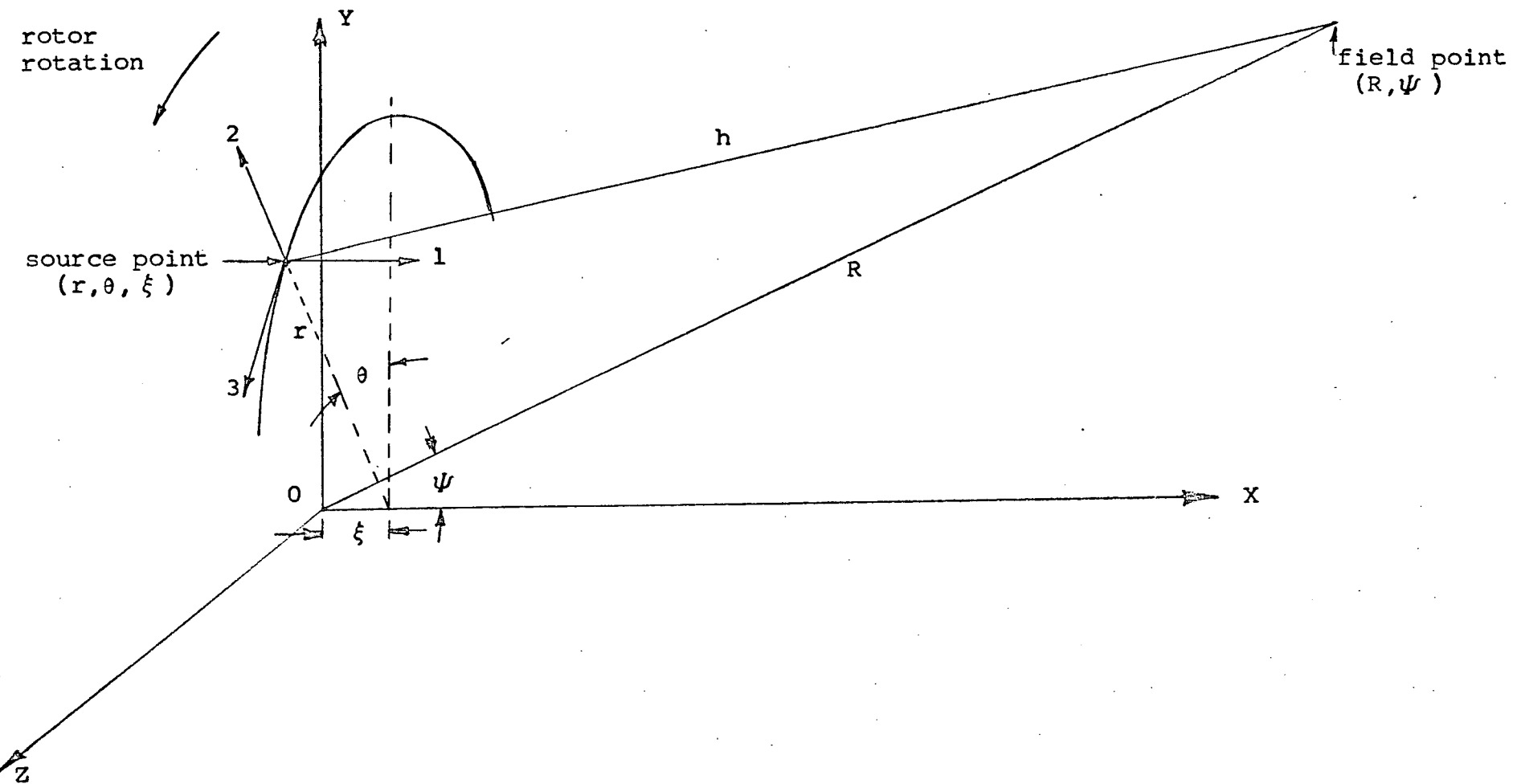


Fig. 1. Field Point Location Relative to the Source Point

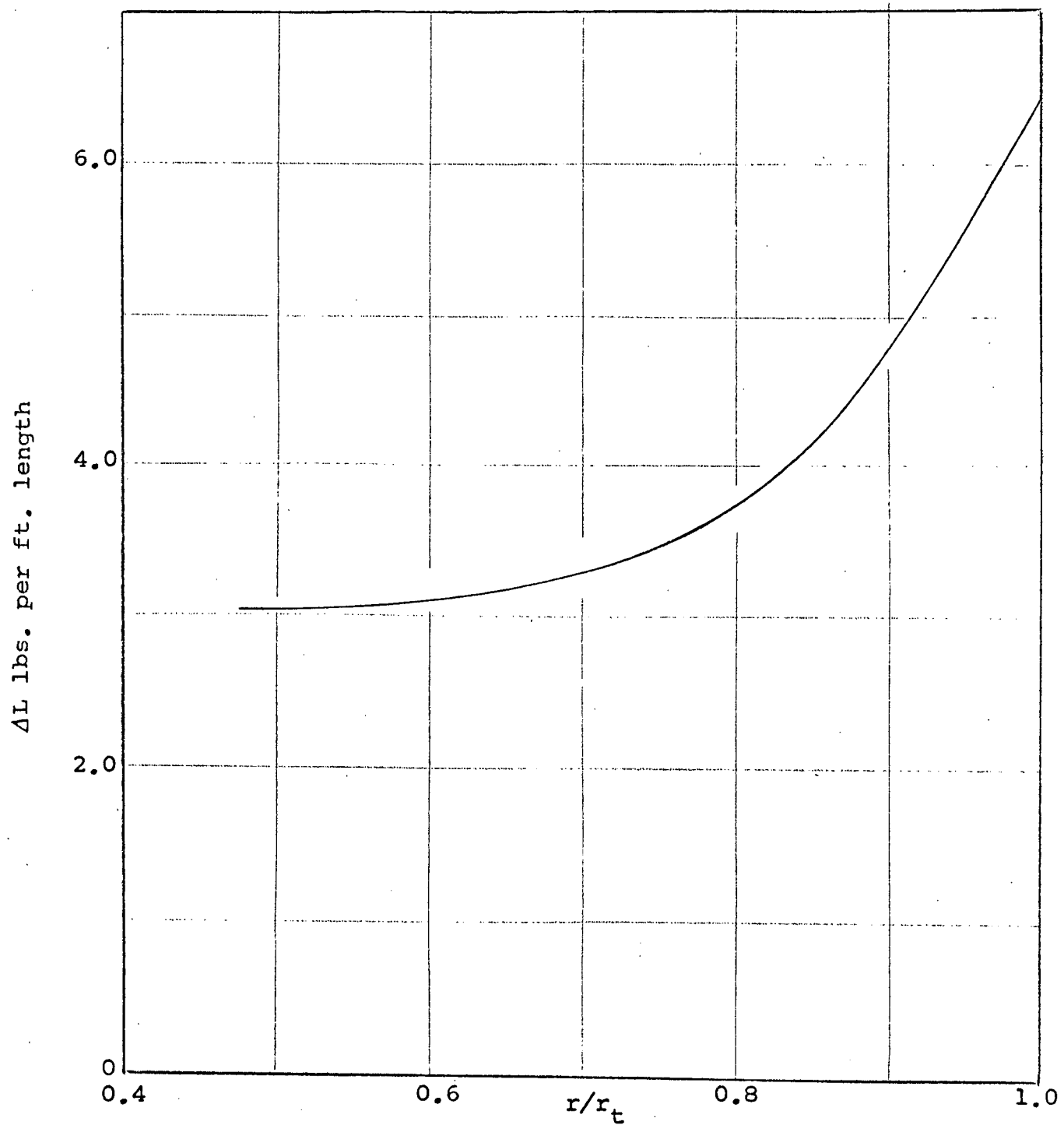


Fig. 2. Steady State Load on Rotor Blade in Rao Fan 2.

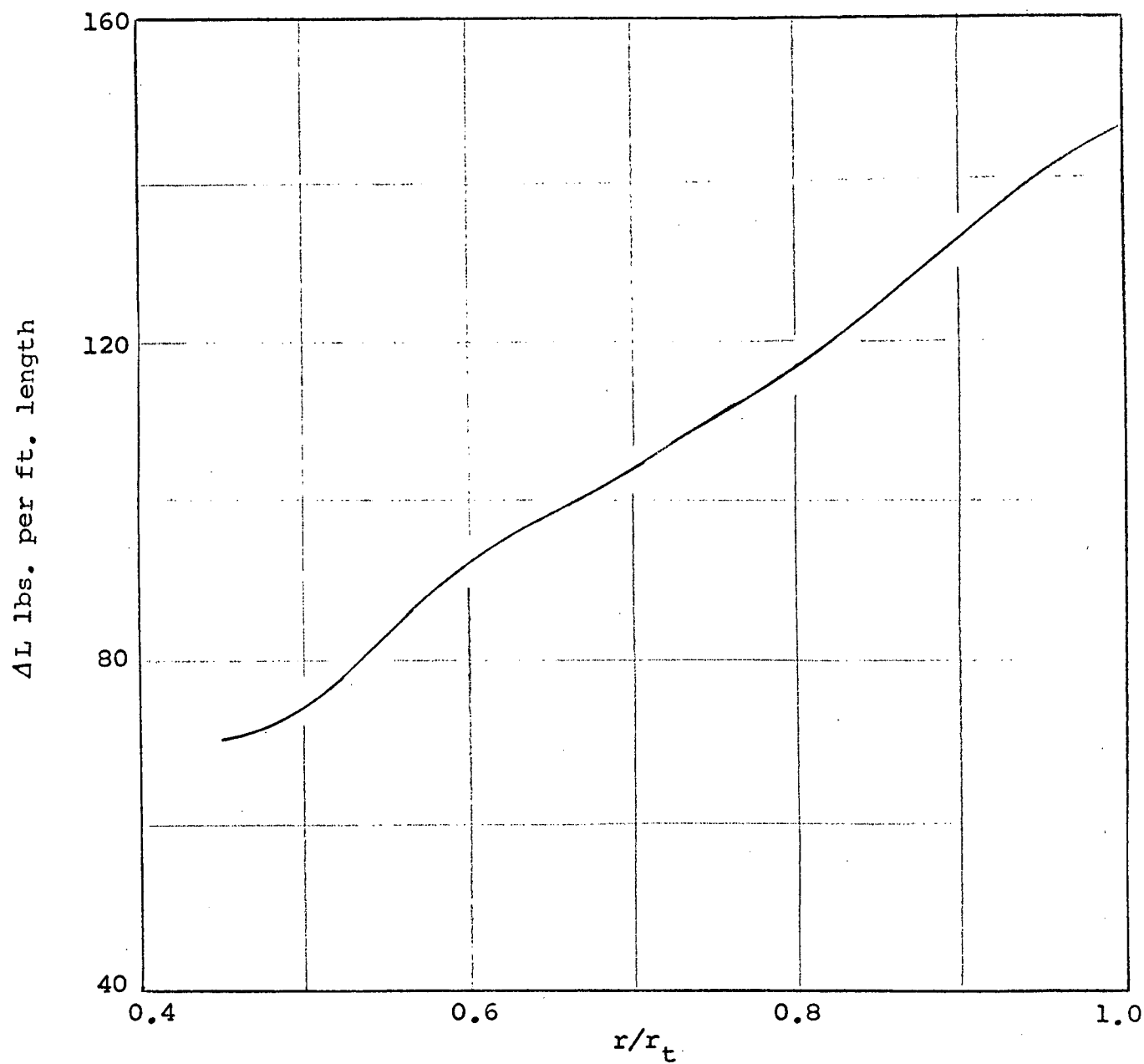


Fig. 3. Steady State Load on Rotor Blade in LF336.

-55-

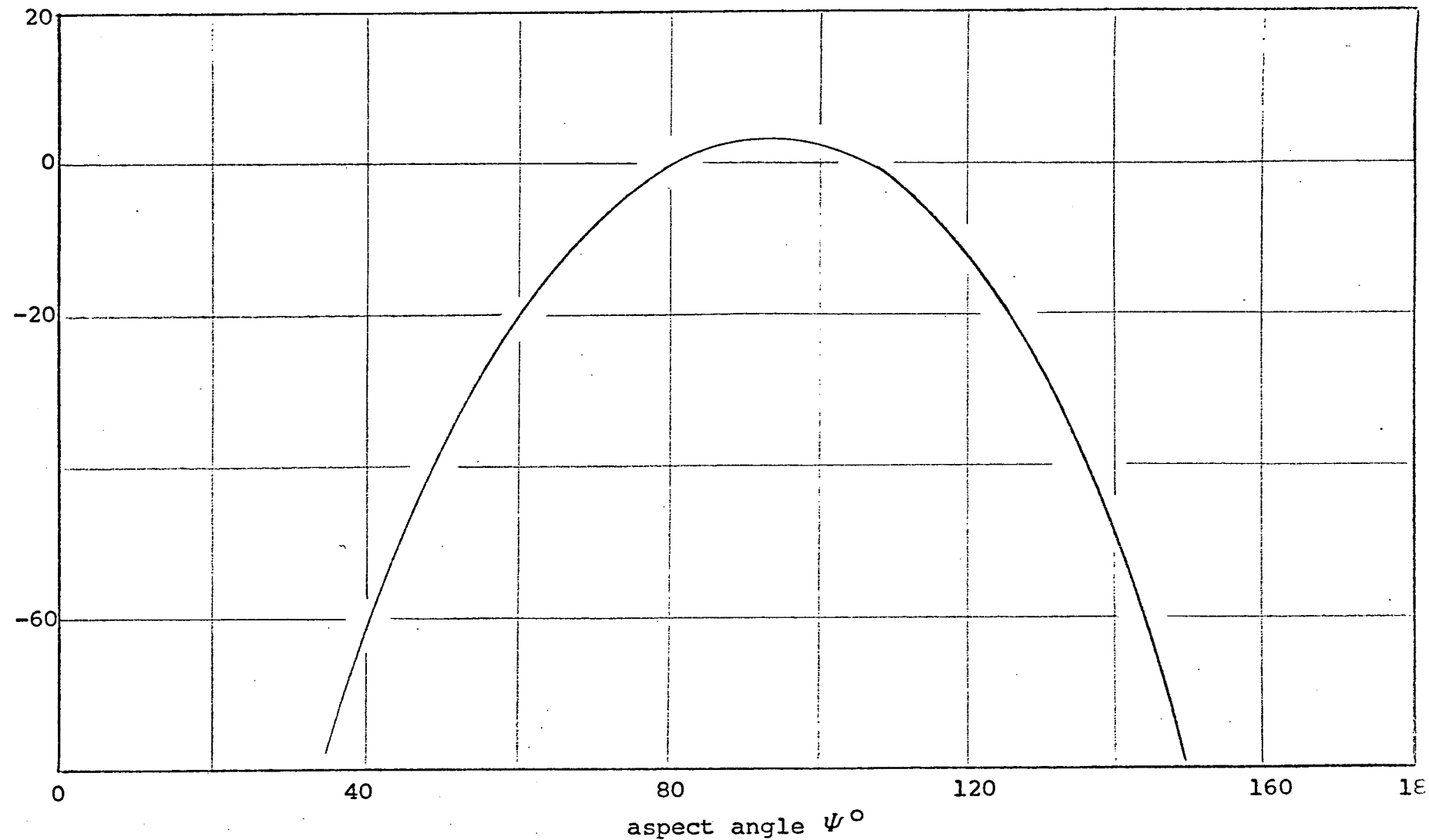


Fig. 4. Sound Pressure Levels at Blade Passing Frequency Computed from Steady State Blade Loading in Rao Fan 2 (5 ft. distance from fan).

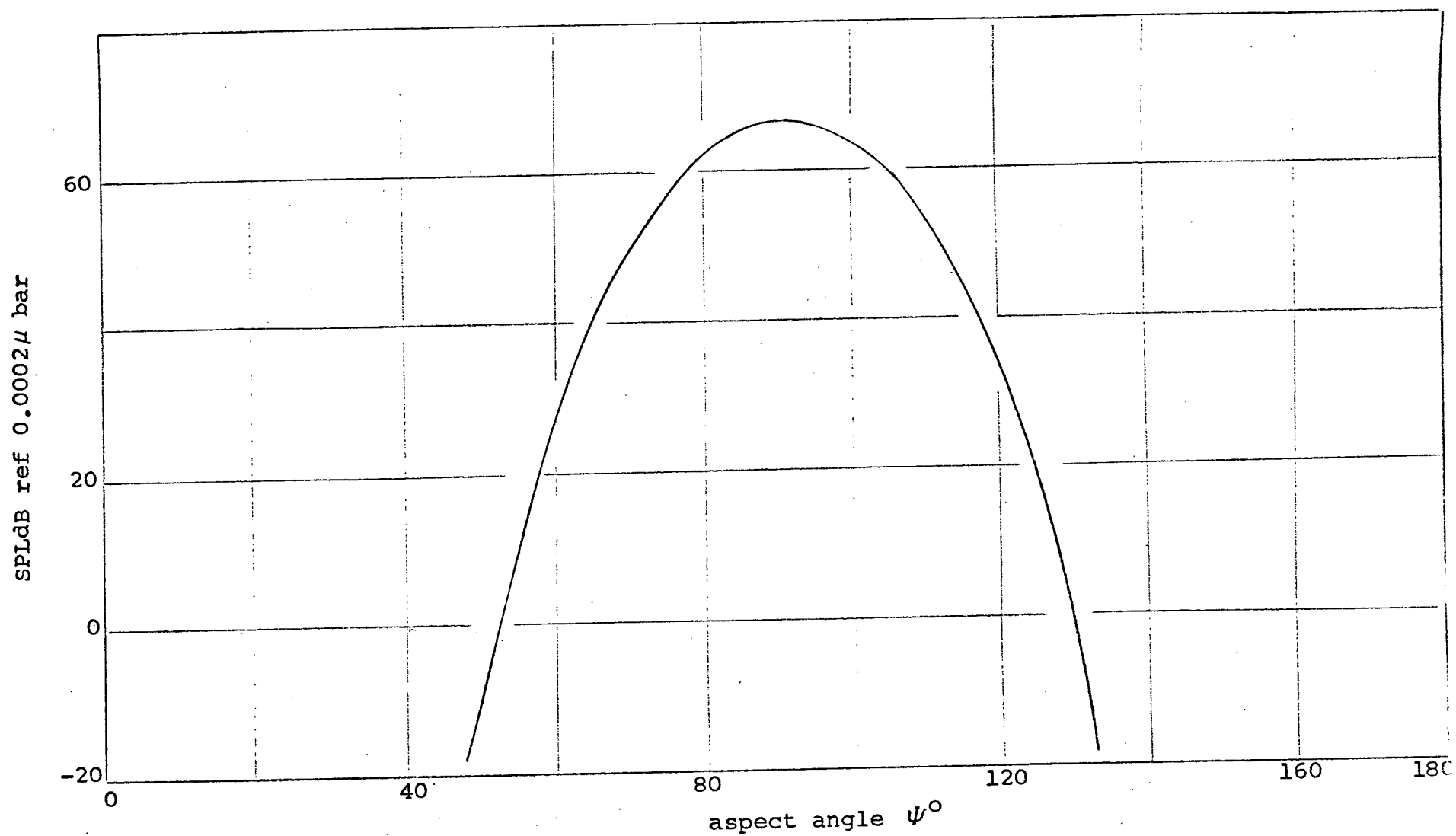


Fig. 5. Sound Pressure Levels at Blade Passing Frequency Computed from Steady State Blade Loading for LF336 (150 ft. distance from fan).

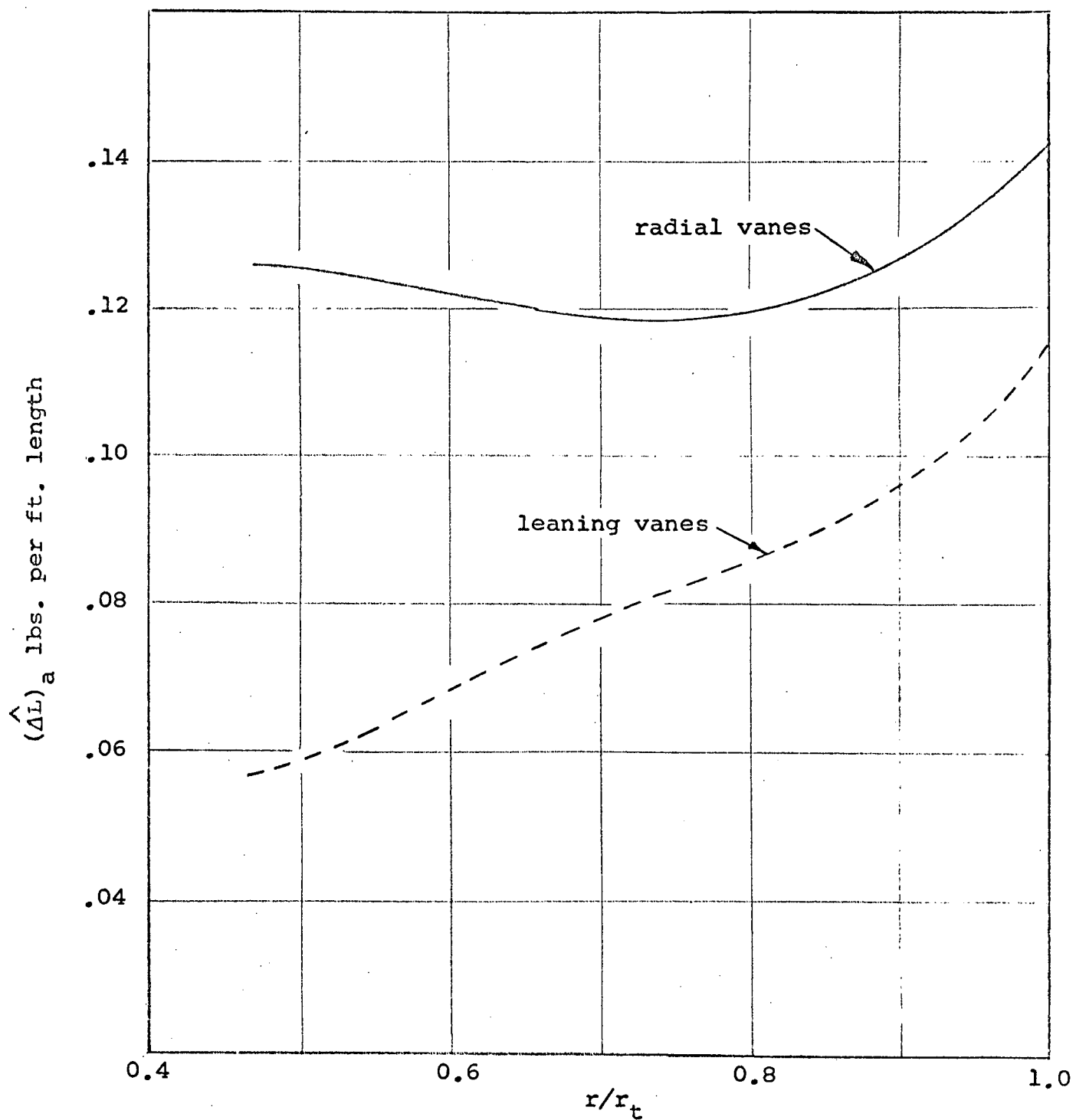


Fig. 6. Radial Variation of Amplitude at Fundamental ($a=1$) of Fluctuating Lift Force on Blade Element in Rao Fan 2.

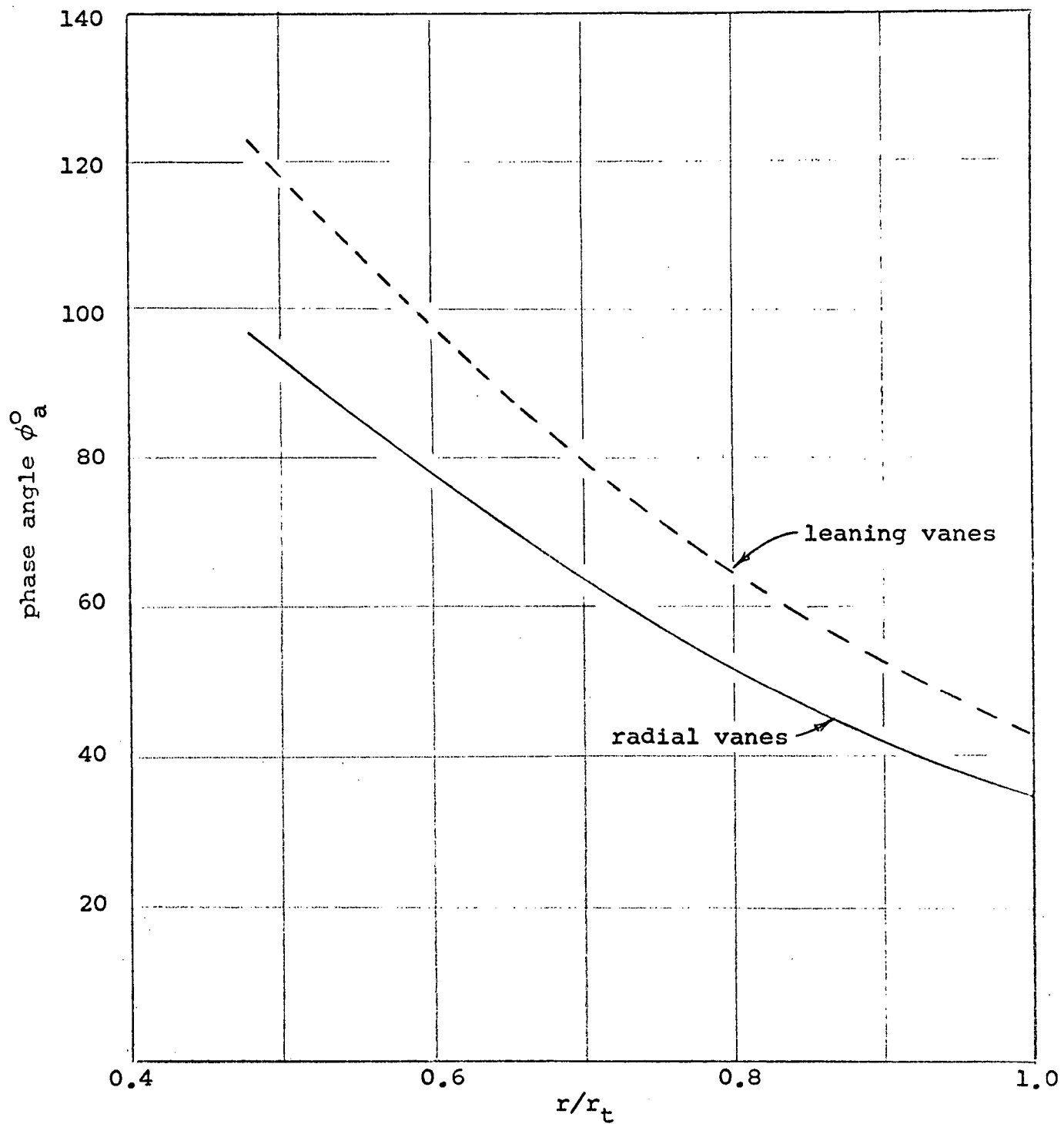


Fig. 7. Radial Variation of the Phase Angle at Fundamental ($a=1$) of the Fluctuating Lift Force on Blade Element in Rao Fan 2.

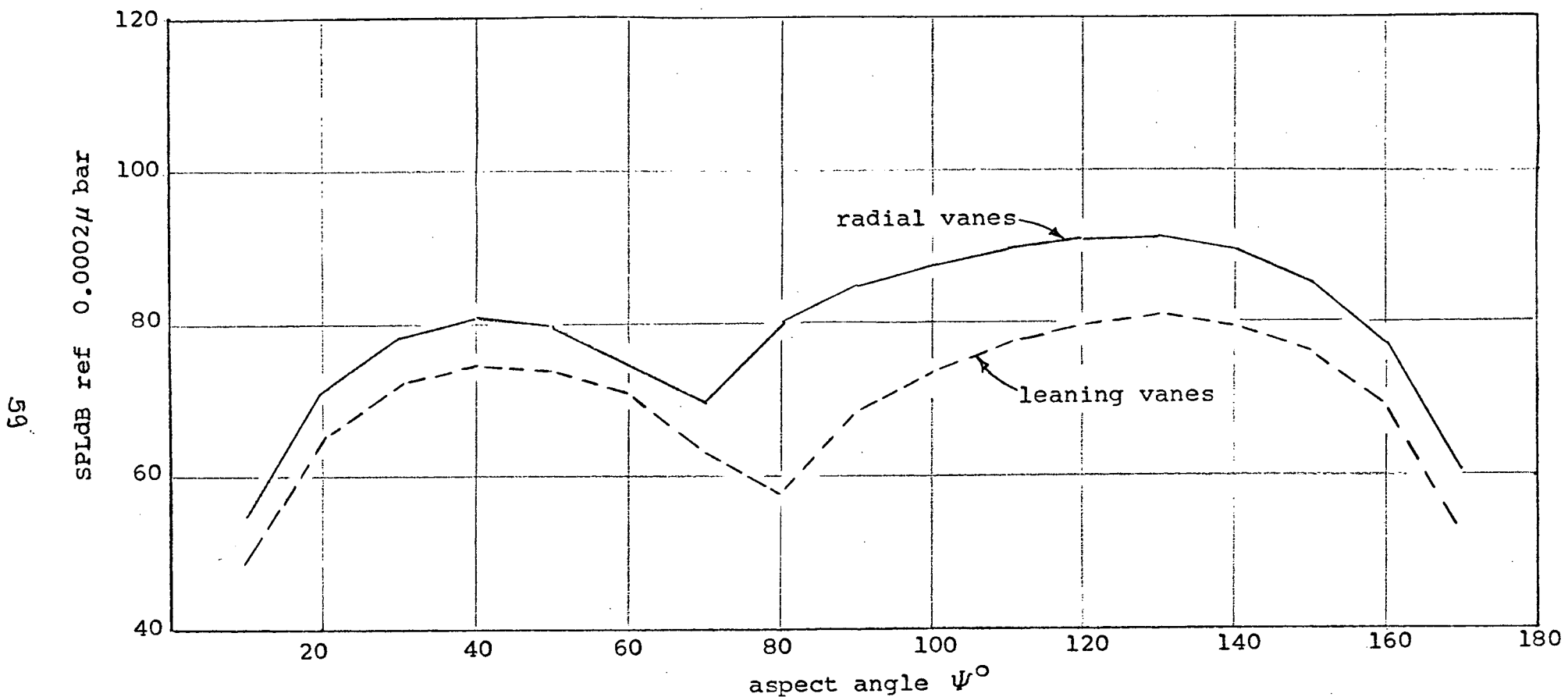


Fig. 8. Sound Pressure Levels at Blade Passing Frequency Computed from Periodic Blade Loading in Rao Fan 2 (5 ft. ditance from fan).

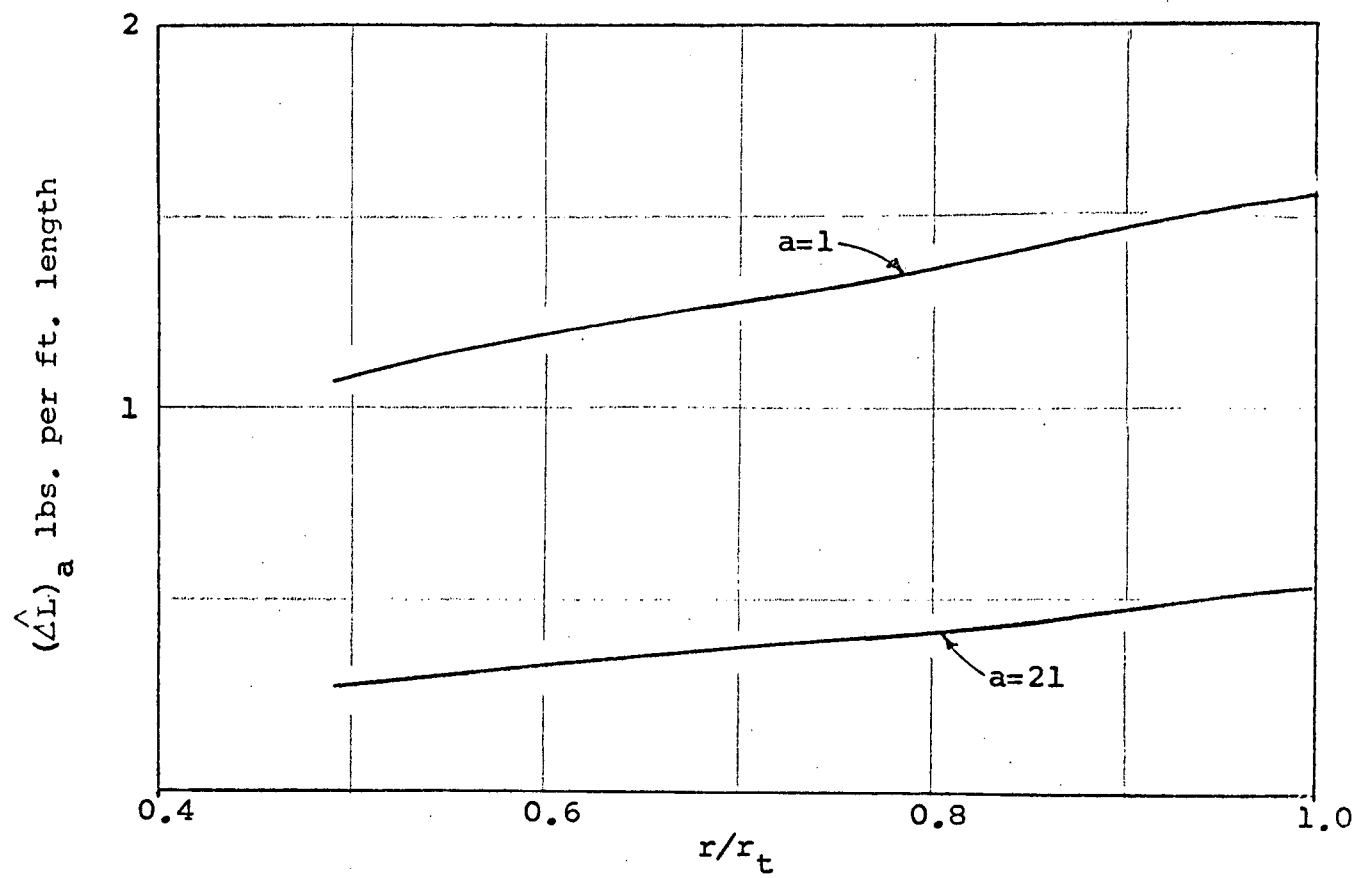


Fig. 9. Radial Variation of a th Component Amplitude of Fluctuating Lift Force on Blade Element in LF336 Due to Major Strut

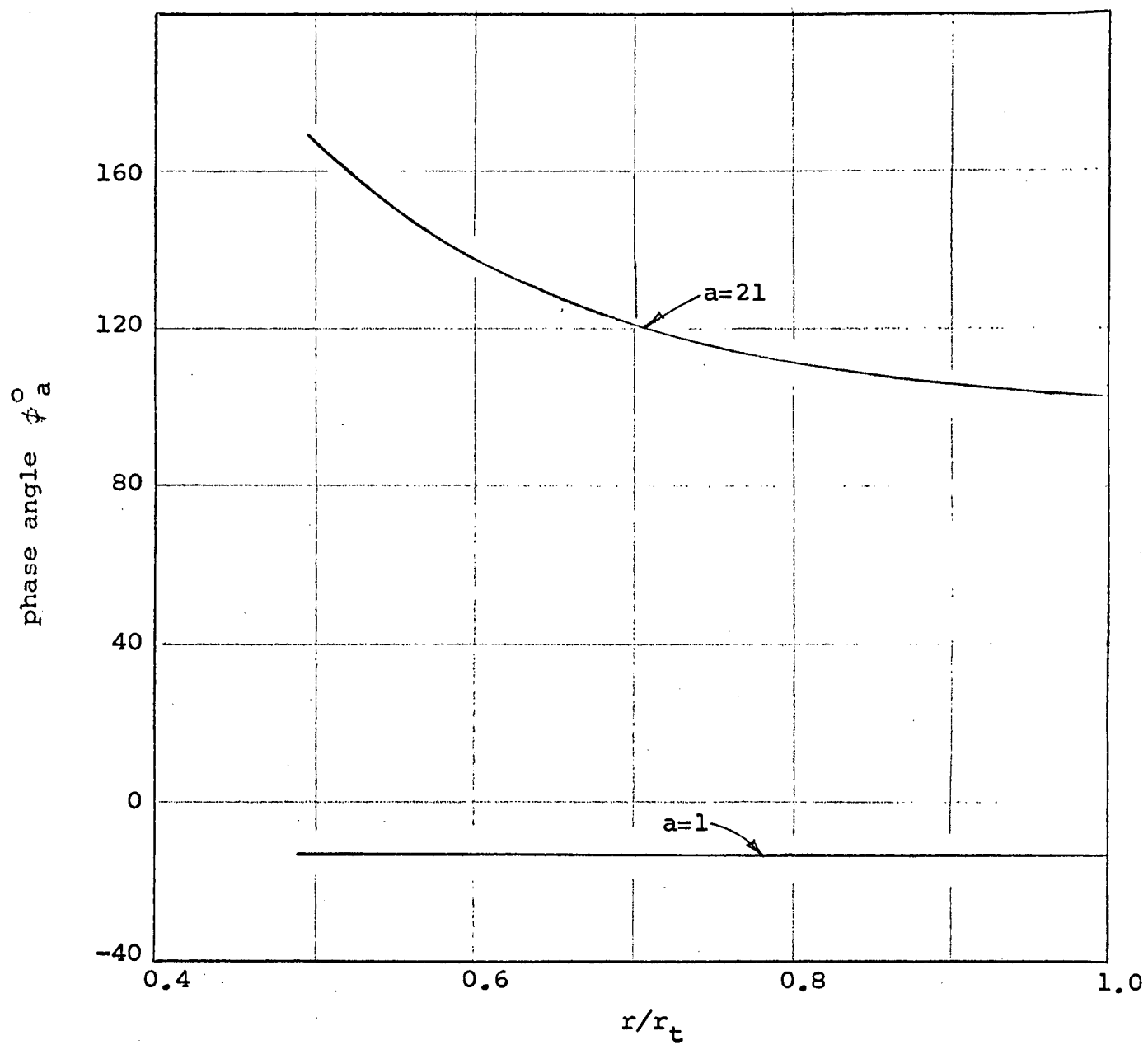


Fig. 10. Radial Variation of a -th Component Phase Angle of Fluctuating Lift Force on Blade Element in LF336 Due to Major Strut

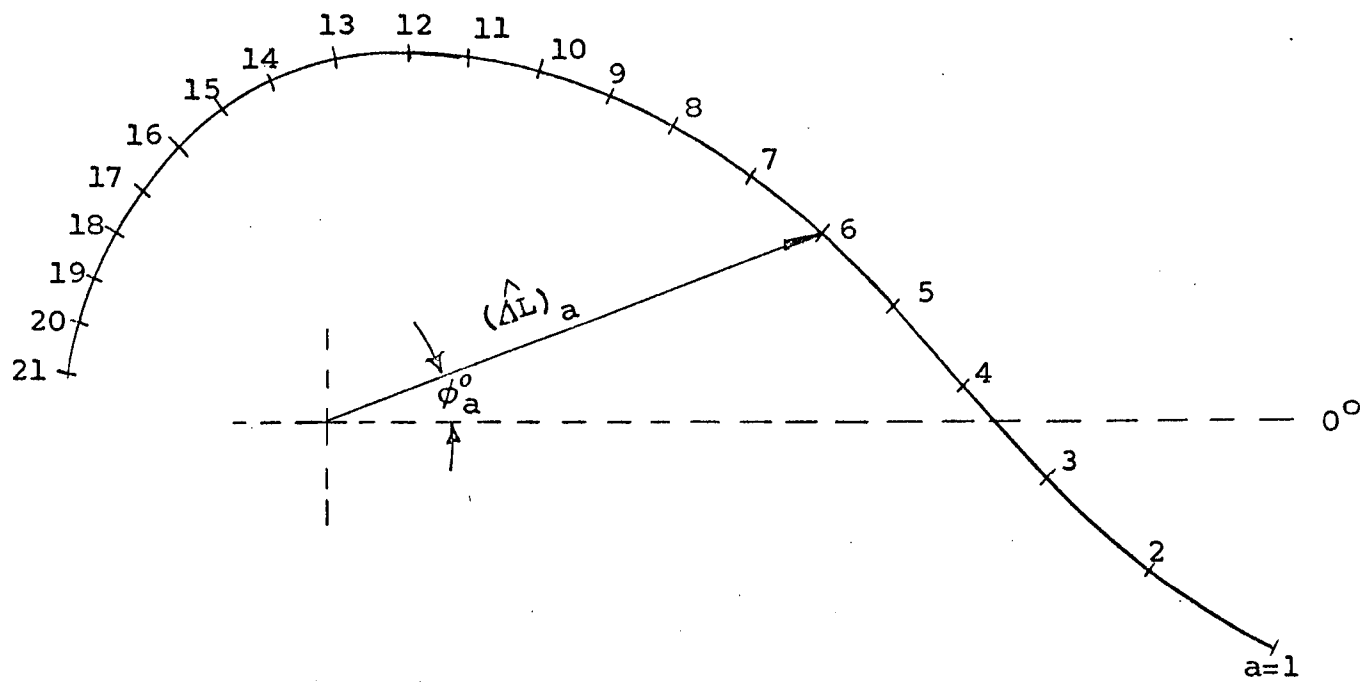


Fig. 11. Vectorial Representation of the a th Component of Fluctuating Lift Force on Blade Element in LF336 Due to Major Strut

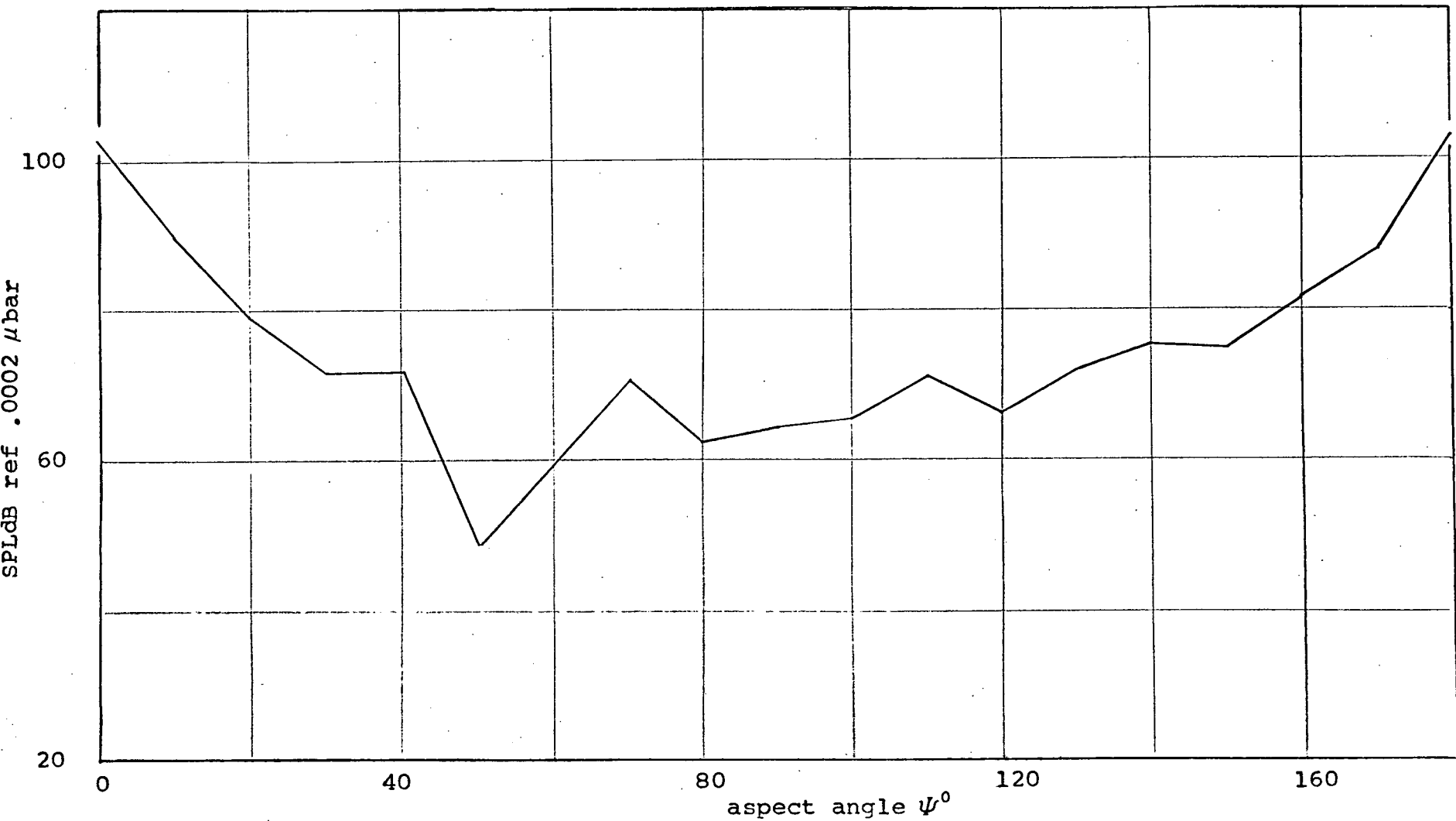


Fig. 12. Sound Pressure Levels at Blade Passing Frequency Computed from Periodic Blade Loading in LF336 at Design Speed
(effect of major strut wake only)

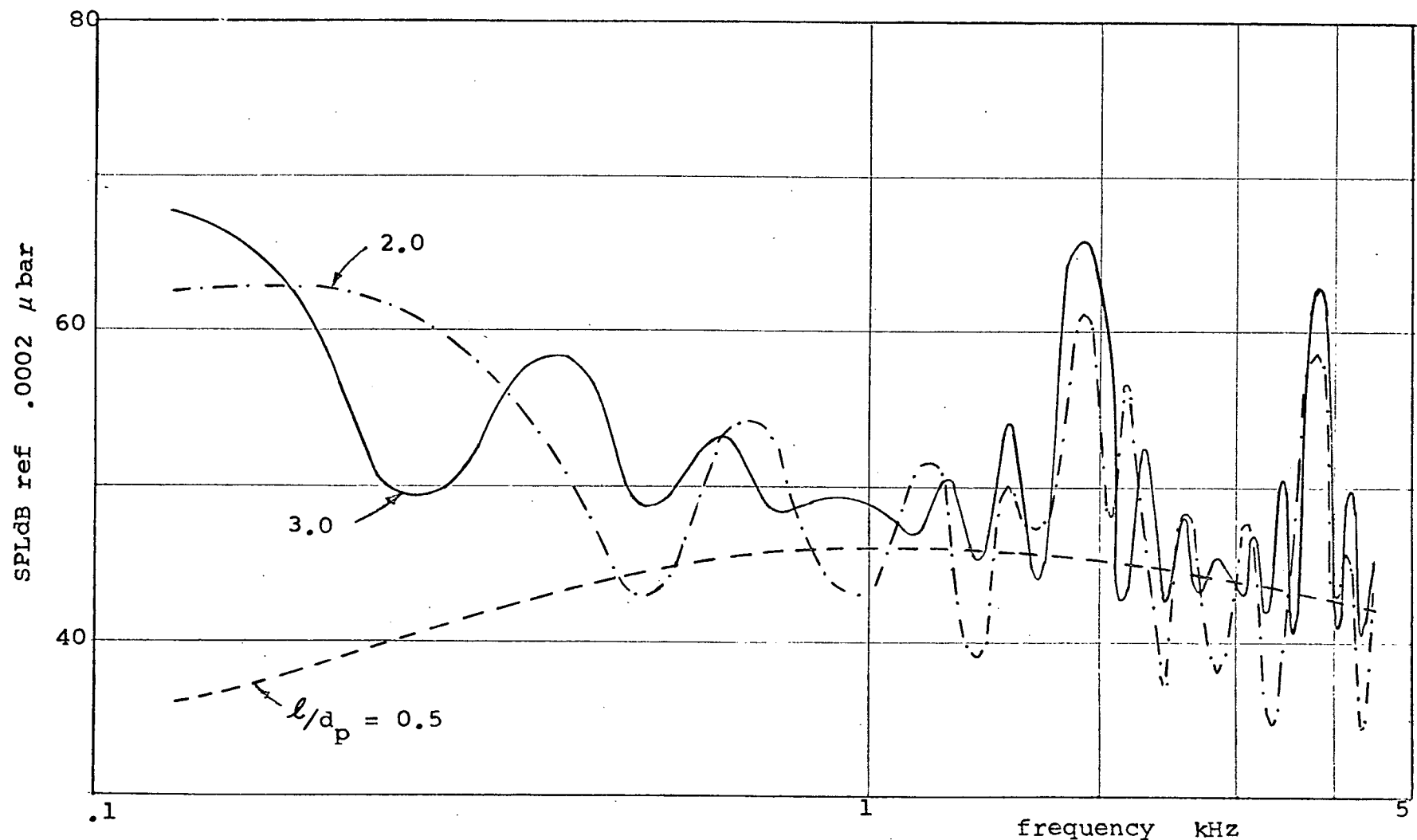


Fig. 13. Acoustic Radiation on the Axis from Random Forces on Rotor Blades
in Rao Fan 2

(inlet turbulence intensity = 3%, distance from fan = 5 ft.)

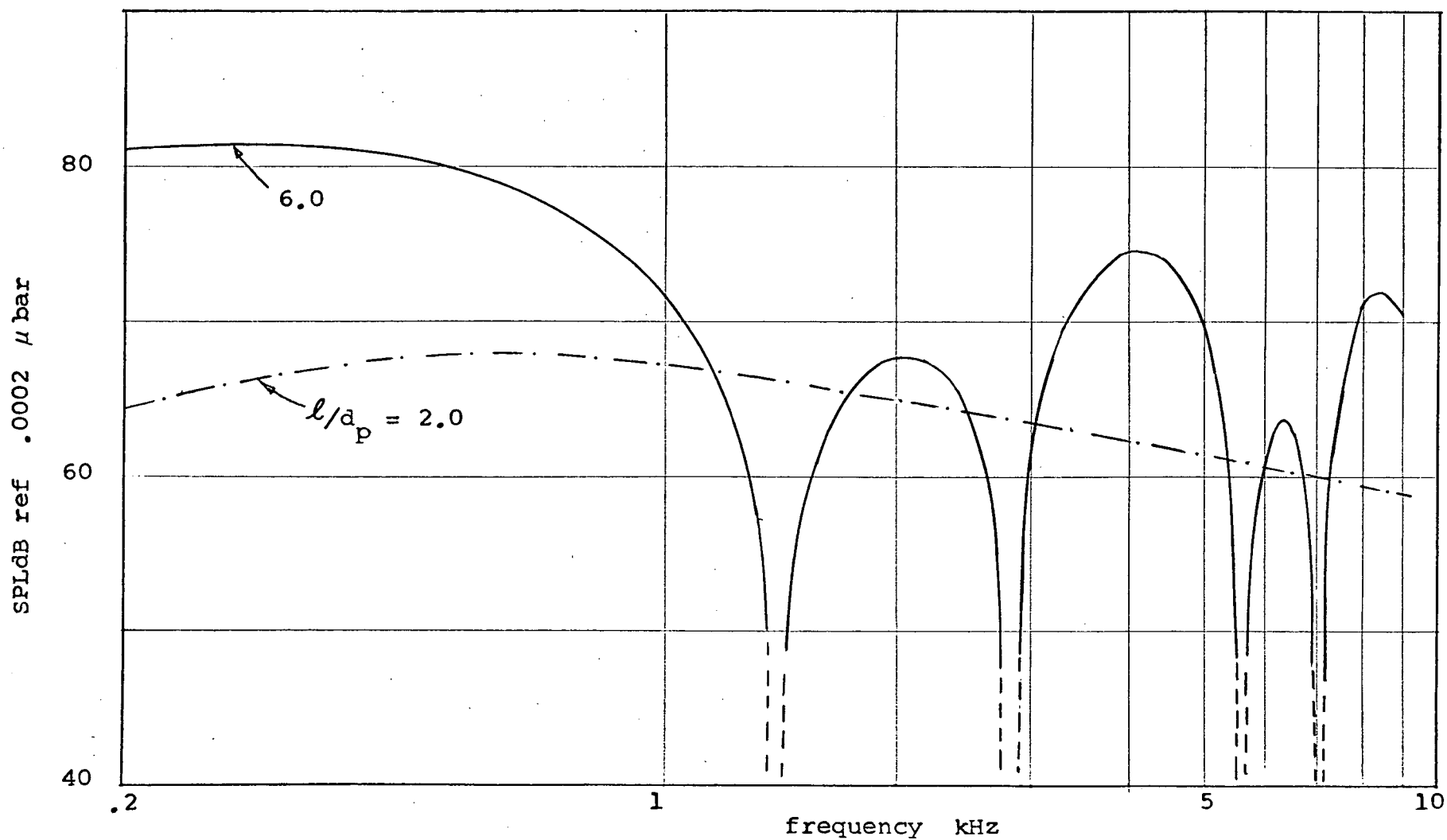


Fig. 14. Acoustic Radiation on the Axis from Random Forces on Rotor Blades
in LF336

(inlet turbulence intensity = 3%, distance from fan = 150 ft.)

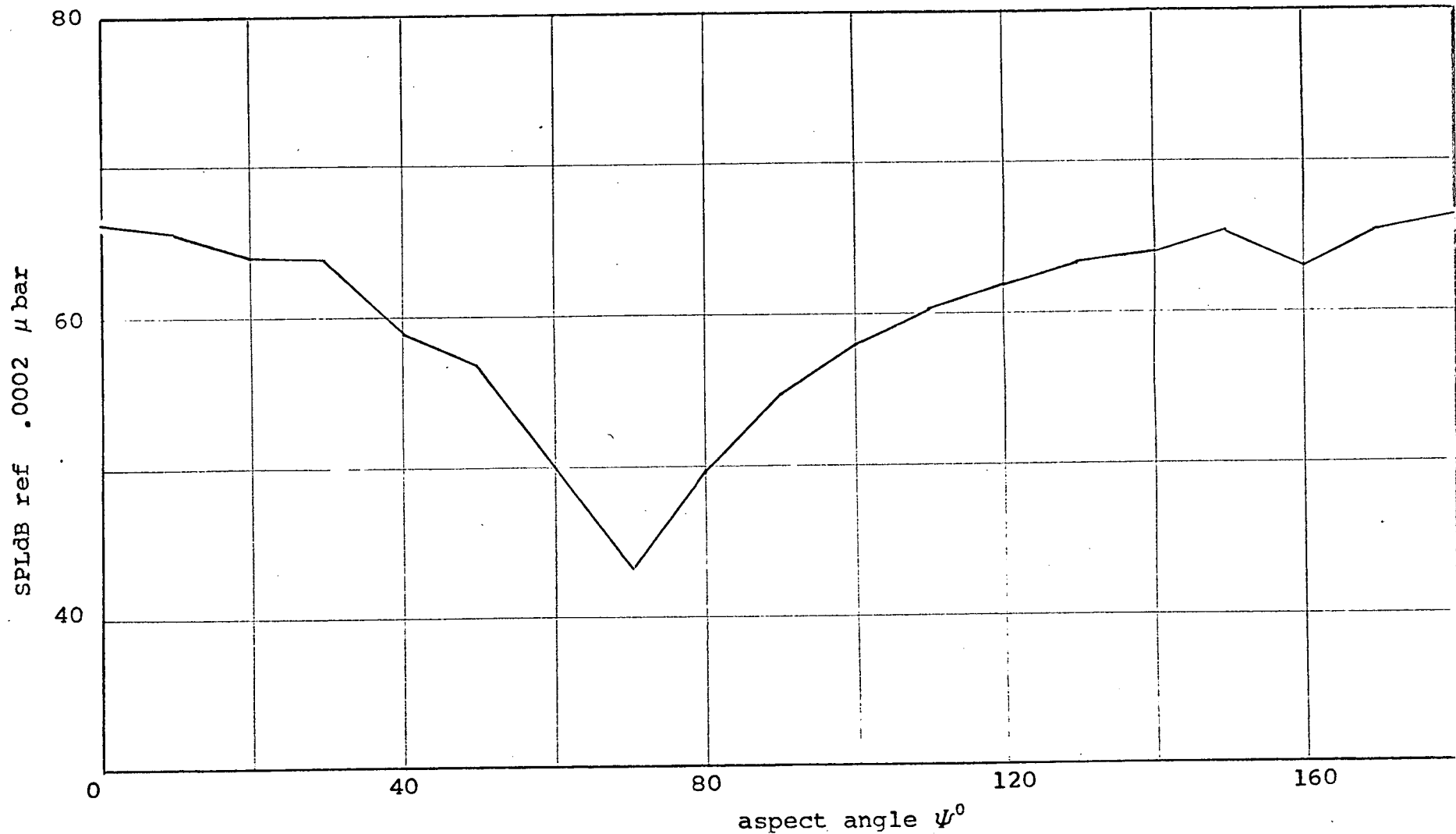


Fig. 15. Directivity of Acoustic Radiation from Random Forces on Rotor Blades
in Rao Fan 2
(turbulence intensity = 3%, $\ell/d_p = 3.0$)

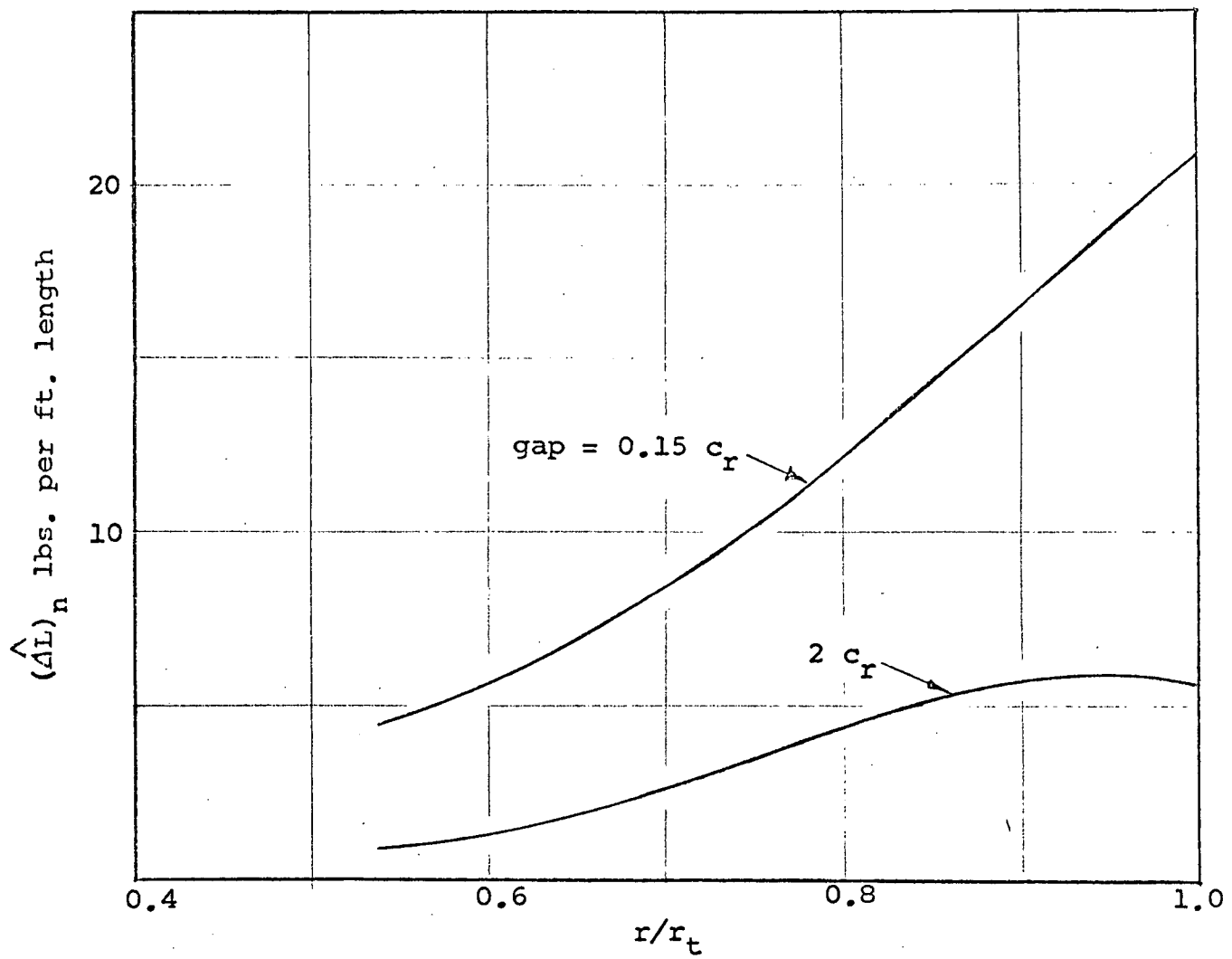


Fig. 16. Radial Variation of Amplitude of Fundamental (n=1) of Fluctuating Lift Force on Vane Element in LF336.

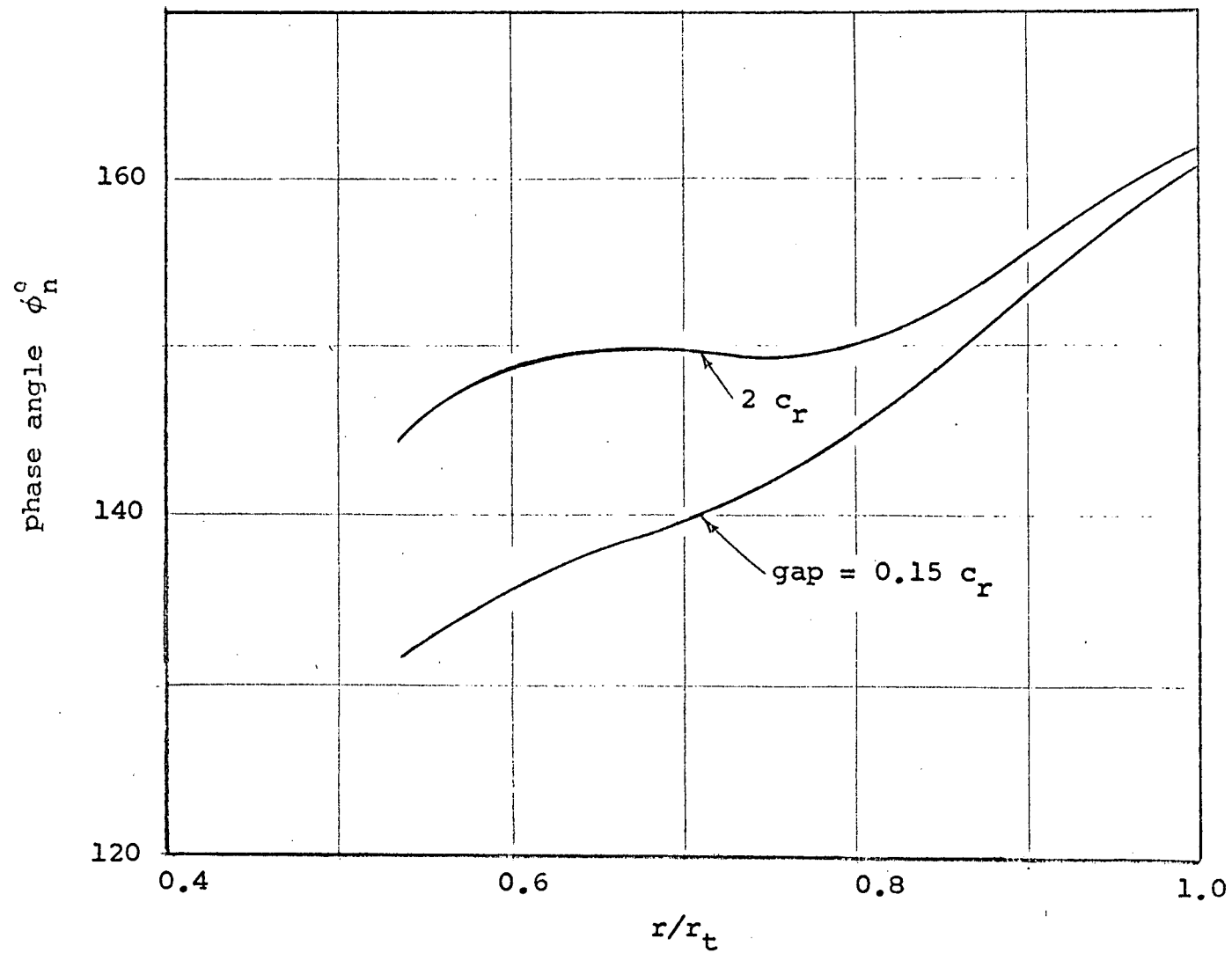


Fig. 17. Radial Variation of Phase Angle of Fundamental (n=1) of Fluctuating Lift Force on Vane Element in LF336.

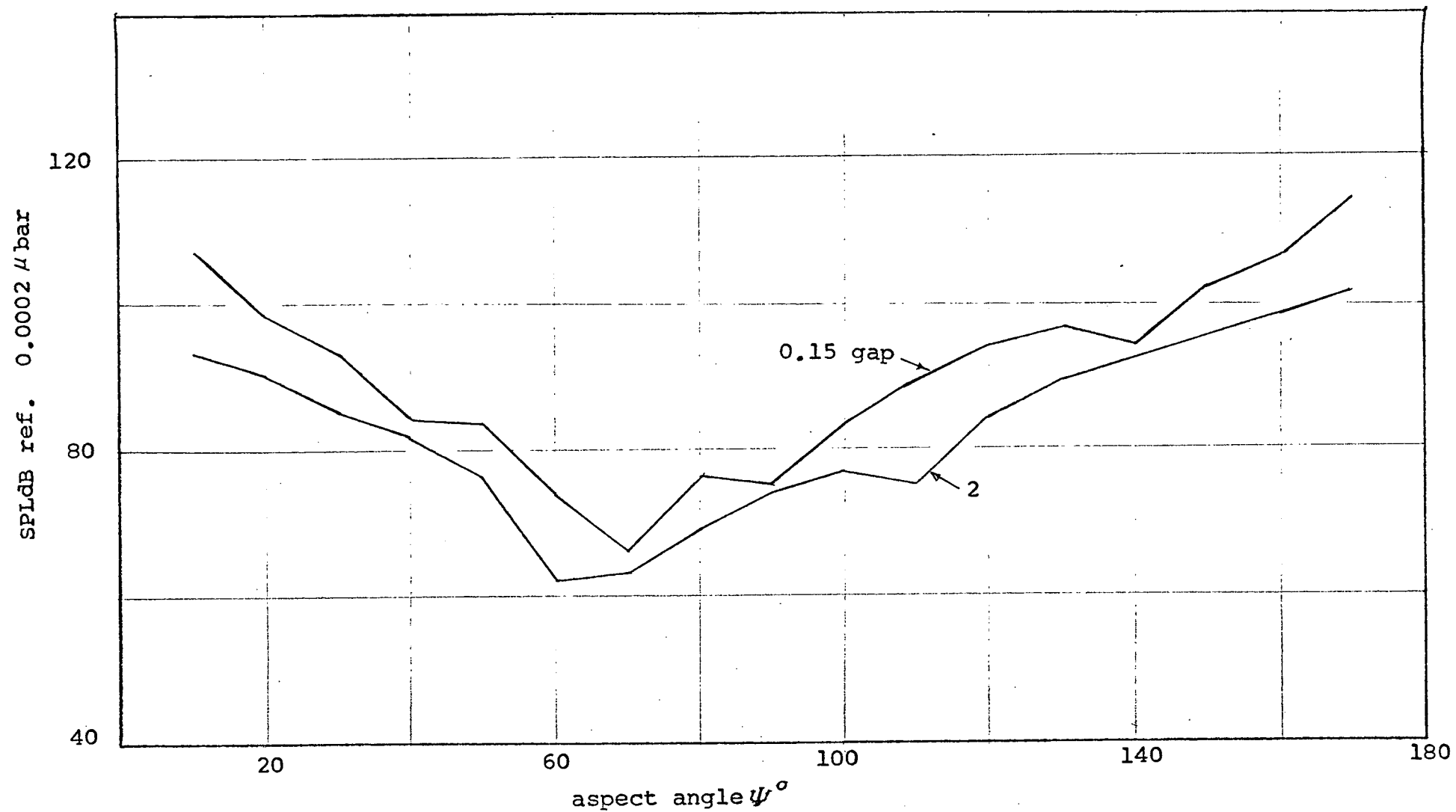


Fig.18. Sound Pressure Levels at Blade Passing Frequency Computed from Periodic Vane Loading in LF336 (150 ft. distance from fan).

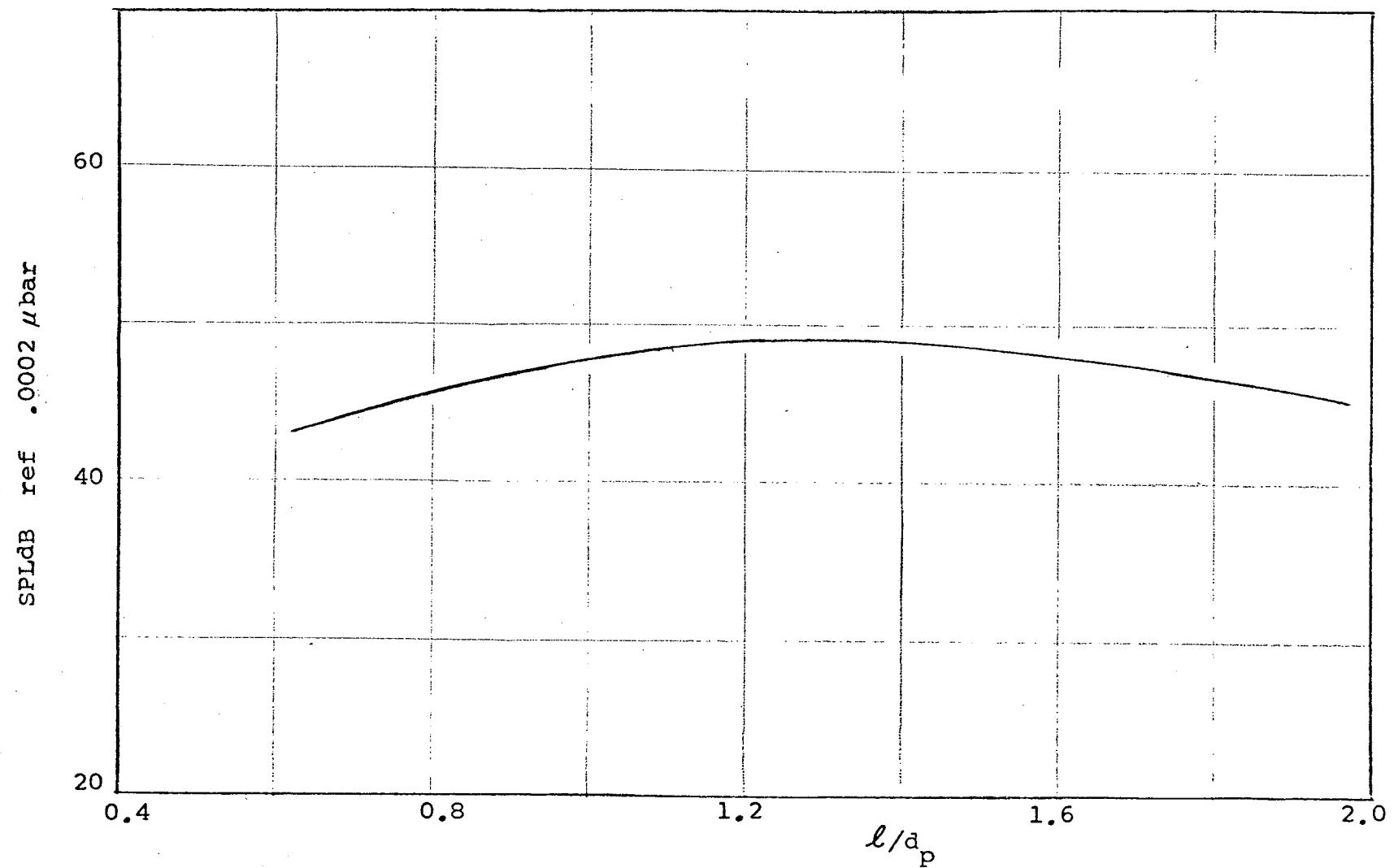


Fig. 19. Acoustic Radiation on the Axis at Blade Passing Frequency from Random Axial- Longitudinal Quadrupoles in Rao Fan 2.
(inlet turbulence intensity = 3%, distance from fan = 5 ft.)